LINEAR ELECTRON ACCELERATOR PROGRESS AT STANFORD UNIVERSITY*

K.L. BROWN, A.L. ELDREDGE, R.H. HELM, J.H. JASBERG,
J.V. LEBACQZ, G.A. LOEW, R.F. MOZLEY, R.B. NEAL,
W.K.H. PANOFSKY, T.F. TURNER
Project M, Stanford University, Stanford, Calif.
(Presented by W.K.H. Panofsky)

I. INTRODUCTION

This report describes progress made during the past several years at Stanford University in certain areas of electron linear accelerator technology. It is a sequel to earlier reports[1,2] presented at the CERN Symposium in 1956 and at the International Conference on High-Energy Accelerators and Instrumentation in 1959. The present document is not intended as a general review of electron linear accelerator problems, nor does it attempt to cover all aspects of accelerator technology studied at Stanford. The intention, rather, has been to describe only certain selected topics and to treat these somewhat more extensively than a general survey would permit.

It will be apparent throughout this article that much of the recent work has been related to the specific design of a 2-mile-long electron linear accelerator. This machine, often called "Project M", would produce a beam of 10 to 20 Bev electrons at an average beam current of 15 to 30 microamps in its initial phase of operation (Stage I). If eventually warranted, these numbers could later be increased to 20 to 40 Bev and 30 to 60 microamps by increasing the number of klystron power sources from 240 to 960 (Stage II). The general appearance of this accelerator laboratory upon completion is shown, as it is presently visualized, in Fig. 1.

Since 1959 a concentrated effort has been made to examine the role of a high-intensity electron linear accelerator operating at energies above the thresholds for creation of all known elementary particles. As a result of these studies, the Stanford machine has been considered "the next logical step" in the accelerator field, and an intensive design and engineering effort is now going ahead.

We shall not discuss in any detail the range of potential experiments that can be carried out with the 2-mile machine; considerable attention has been paid to analyzing specific "thought experiments" in sufficient detail[3] to give guidance to both accelerator and target area design. The latter is described in the last section of this article. The principal change, since earlier reports, in the prospective research use of the machine has resulted from re-analysis of secondary-particle yields: these studies have placed secondary-particle experiments (including neutrino experiments) in a considerably more favorable position than previously.

II. GENERAL DESIGN CONSIDERATIONS FOR THE TWO-MILE MACHINE

As noted above, much of the work reported in this article, although applicable to the electron linear accelerator field in general, is directly aimed at the design of the Stanford 2-mile machine. In order to tie these various topics together, it appears logical to begin with a brief description of the major design considerations and specifications of the 2-mile accelerator.

A linear accelerator for relativistic electrons differs from circular accelerators in that there are a large number of fairly independent parameters to be chosen. A number of these parameters will strongly affect the research uses of the machine; therefore, it is desirable to attempt to take future experiments into account much

* This work was supported by the United States Atomic Energy Commission.

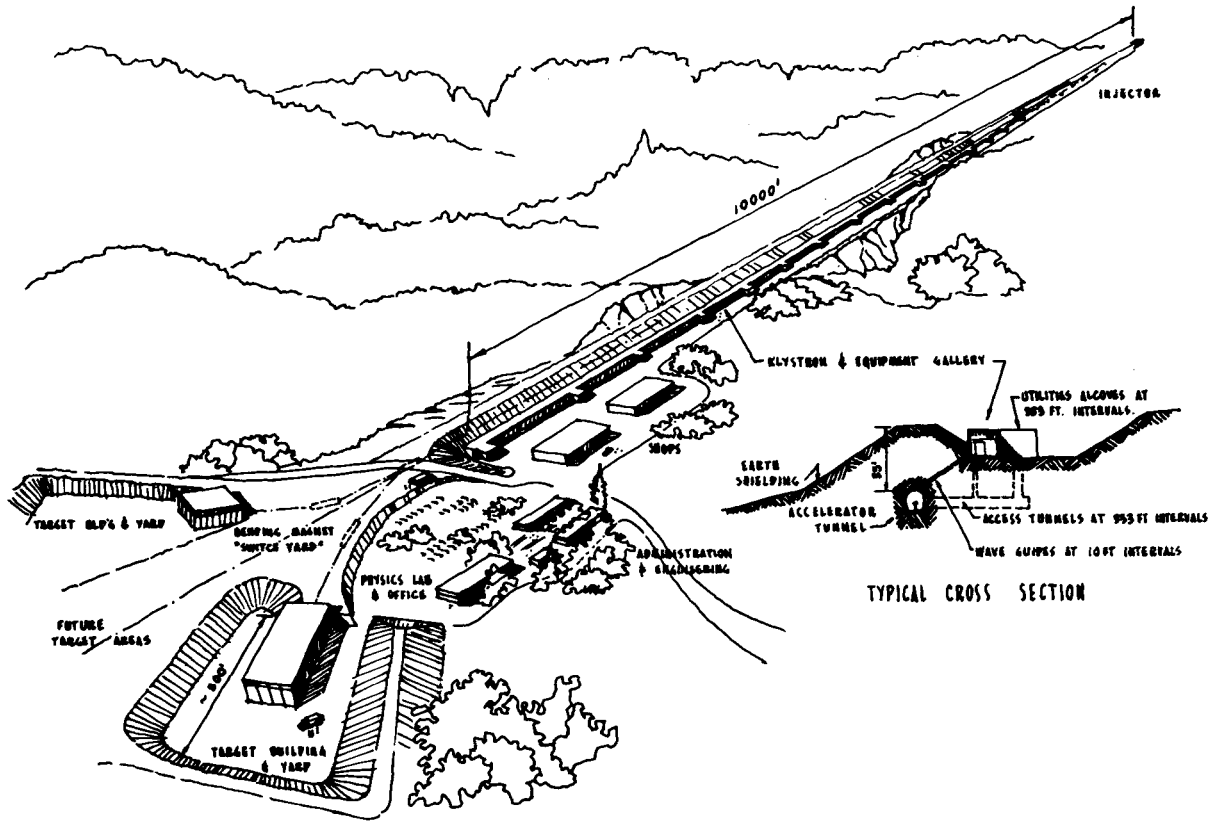

Fig. 1 General view of the accelerator laboratory as presently conceived.

more than is usually the case in the early phases of machine design. The final choice of parameters, however, often involves compromises between future research utility and economic considerations.

A fundamental parameter is the *power-to-length ratio*, which is primarily determined by economic rather than technical considerations. For the M accelerator this ratio has been chosen initially at such a low value that voltage breakdown in the accelerating structure should not be a problem; such a low gradient will make it possible to increase the beam energy at a later date, should this be warranted. In its initial stage of operation (Stage I), the M accelerator will be equipped with 240 klystron amplifiers, each capable of supplying 24 Mw of peak power. These tubes will be spaced at 40-foot intervals along the length of the accelerator, and the power from each tube will be split into 4 equal parts and will feed 4 successive 10-foot accelerator sections. Provisions are made in the initial design to permit later connection, with a minimum of lost research time and equipment obsolescence, of a total of 960 klystrons to the accelerator (Stage II). Thus, in the Stage II design, one klystron will be connected to each 10-foot accelerator section, and the maximum energy and beam current will be twice the Stage I values.

A high *operating frequency* is preferred on the basis of improved shunt impedance per unit length (hence, less rf power requirement and lower cost), decreased filling time, higher permissible electric field strength, and less stringent relative (but not absolute) frequency and dimensional tolerances. On the other hand, lower frequencies are preferable on the basis of higher maximum beam currents, larger beam apertures, and the higher power available from individual rf sources. The Project M accelerator will operate at S-band ($\lambda = 10.5$ cm); this represents a compromise among the factors noted above.

A *traveling-wave* rather than a standing-wave accelerating structure has been chosen because of the greater ease of feeding rf power to the former and its more precise attainment of equilibrium conditions.

The $2\pi/3$ *operating mode* (3 loading disks per wavelength) has been chosen (see Section IV.B) in preference to the previously used $\pi/2$ mode (4 disks per wavelength), because the former has somewhat higher shunt impedance and, because of the fewer disks, it is less costly to construct and has superior vacuum-pumping qualities.

Both *constant-attenuation* and *constant-gradient* designs of accelerating structures are still being evaluated. Because of its uniform physical construction the former would be easier and cheaper to build. However, the latter has higher ultimate energy capability, and because of its nonuniform modular construction may be less subject to beam blow-up (see Section III. D. 3) at very high beam currents.

Whichever of the structures mentioned in the last paragraph is chosen, it will be designed for a lower value of the *attenuation parameter* ($\alpha\ell \cong 0.57$) than earlier Stanford accelerators. The small sacrifice in no-load energy thus incurred will be more than compensated by the decreased filling time, decreased beam-loading effect on energy, decreased transient-energy spread, higher maximum current, reduced frequency sensitivity, and lower energy loss in unpowered sections.

The choices of *repetition rate* and *rf pulse length* primarily involve compromises between the data rate and the costs associated with such items as higher modulator power and water cooling. The highest repetition rate is clearly desirable for experimental purposes; a rate (360 pulses per second maximum) has been chosen at which the modulator input power becomes comparable to the fixed-power requirements such as lighting, cathode power, target-area requirements, etc. The rf pulse length (2.5 μsec) has been chosen so that the time available for beam acceleration is roughly twice the filling time of the accelerator. As a result of these choices, the M accelerator will have an order of magnitude better beam duty-cycle (6×10^{-4}) than the present 1-Bev accelerators at Stanford and Orsay.

Because of the anticipated large demand for operating time, the M accelerator has been designed to operate 24 hours per day for extended periods. This specification has imposed stricter design requirements than were encountered in earlier linear accelerators, such as the need for capability of servicing and replacing components (e.g., klystrons) without interference with research utilization of the machine.

The principal specifications of the M accelerator are given in the following table (Table 1).

TABLE 1

PRINCIPAL M ACCELERATOR SPECIFICATIONS

	Stage I	Stage II
Accelerator length	10,000 feet	10,000 feet
Length between feeds	10 feet	10 feet
Number of accelerator sections	960	960
Number of klystrons	240	960
Peak power per klystron	6–24 Mw	6–24 Mw
Beam pulse repetition rate	1–360 pps	1–360 pps
RF pulse length	2.5 μsec	2.5 μsec
Electron energy, unloaded	11.1–22.2 Bev	22.2–44.4 Bev
Electron energy, loaded	10–20 Bev	20–40 Bev
Peak beam current	25–50 ma	50–100 ma
Average beam current	15–30 μa	30–60 μa
Average beam power	0.15–0.6 Mw	0.6–2.4 Mw
Filling time	0.83 μsec	0.83 μsec
Electron beam pulse length	0.01–2.1 μsec	0.01–2.1 μsec
Electron beam energy spread (max)	$\pm$ 0.5%	$\pm$ 0.5%
No. of electron energy levels	up to 6	up to 6
Accelerator vacuum	$<10^{-5}$ mm of Hg	$<10^{-5}$ mm of Hg
Operating frequency	2,856 Mc/sec	2,856 Mc/sec
Operating schedule	24 hrs/day	24 hrs/day

III. BEAM DYNAMICS

The beam dynamics study in connection with the Project M accelerator is concerned primarily with the problems, arising in an extremely long linear accelerator, which affect the beam transmission and the final transverse momentum and energy spectrum of the beam. In particular, it is necessary to examine those factors where experience with the present 1 Bev machine (Mark III) may not be sufficient to give confidence in the behavior of a 2-mile machine.

A. "Ideal" Machine

We consider first an ideal machine, defined as follows:

(1) The rf field is circularly symmetric, synchronous with the beam, and of constant strength in the longitudinal direction.
(2) The machine is perfectly straight.
(3) There are no external magnetic fields.
(4) Space-charge forces (i.e., beam-current-dependent effects) are negligible.

There is also an implicit assumption that the beam is injected into the machine at a highly relativistic energy.

Such a machine is characterized by a rapid decrease as a function of length of transverse forces and longitudinally dispersive forces, because of relativistic effects and the cancellation of transverse electric and magnetic forces in a TM wave at a phase velocity equal to the velocity of light. By the time the energy reaches a few Mev, the electron bunches are essentially frozen in phase by the large increase in "longitudinal mass", and no further bunching or debunching occurs; energy increases linearly with length; transverse momentum becomes constant because of the vanishing of transverse forces; and all coupling between longitudinal and transverse coordinates becomes negligible.

The constant transverse momentum and linearly increasing energy result in the angular divergence of the beam decreasing inversely with length, and logarithmically increasing beam radius. The spread in transverse momentum introduced in the injector is estimated at $\sim \pm 0.1$ (in units of mc) which with injection at 60 Mev and a final energy of 15 Bev would introduce an increase in radius of 5.5 cm if no focusing were used. A system of quadrupoles each of about 1,000 gauss strength, with a spacing of four quadrupoles per two-fold energy increase, would be appropriate in the above example to keep the orbit amplitudes within about half the radius of the accelerator hole.

B. Non-Ideal Conditions

Several effects which will exist in a real machine may lead to deterioration in beam quality or decrease in transmission. Some of these are:

(1) Longitudinal variations in rf phase and amplitude.
(2) Asymmetry in the rf field.
(3) Stray magnetic fields.
(4) Accelerator misalignments (deviation from straightness).

1. Longitudinal Variations

The rf field variations introduce a force which may be expressed, to first order in the transverse coordinates, as

$$\frac{dp_r}{dz} = -\frac{r}{2}\left(\frac{1}{\beta_e}\frac{\partial}{\partial z} + \frac{\partial}{\partial t}\right) E(z,t) \quad (1)$$

where $E(z,t)$ is the traveling-wave accelerating field at the accelerator axis; p_r is the radial momentum; z and r are respectively the longitudinal and radial distances; β_e is the normalized electron velocity; t is the time [in a system in which momenta are expressed in units of mc; r and z are in units of c/ω; t is in units of $1/\omega$; and electric and magnetic fields are in units of $(\omega/c)mc^2/e$, which is equivalent to 1,020 gaussian units or 306 kv/cm].

The effect of asynchronism averages to zero (to first order in E) in a relativistic machine, as do small random longitudinal variations in field strength. The fringe-field at the end of the machine contributes a thin (diverging) lens effect, which however is negligible since the focal length turns out to be approximately twice the length of the machine.

Periodic variations, such as would be introduced by the loading disks and periodic power feeds, introduce a small residual focusing force quadratic in the accelerating field strength, of the form

$$\frac{dp_r}{dz} \cong -\frac{r}{4P}\left(\overline{E^2} - \bar{E}^2\right) \quad (2)$$

where P is longitudinal momentum, and $(\overline{E^2} - \bar{E}^2)$ is the mean square deviation of the accelerating field seen by an electron. The effect is thus equivalent in focusing strength to an *axial magnetic field* of magnitude $\sqrt{\overline{E^2} - \bar{E}^2}$; for Project M design, Stage I (15 Bev), this amounts to approximately 80 gauss, which implies a negligibly small focusing force. Thus, nonlinear effects arising from longitudinal rf field variations can probably also be safely ignored.

2. *RF Field Asymmetry*

Asymmetry of the rf field, such as might arise in the power couplers, will introduce a transverse deflecting force proportional to the transverse gradient of the rf vector potential; i.e.,

$$\frac{dp_x}{dz} \cong \frac{\partial}{\partial x}\frac{\partial E}{\partial t} \tag{3}$$

in the system of units introduced in the preceding section. The net deflection of such a force could be cancelled by magnetic steering. However, phase spread of the electron bunches is coupled into the transverse momentum, leading to an increase in final angular divergence. A final angular divergence of about 10^{-5} radian implies a transverse field variation (normalized to the length of one coupler cavity) of not more than $\sim$0.5 percent across the diameter of the accelerator aperture. By way of comparison, couplers now in use in existing Stanford machines have a variation of $\sim$12 percent across the coupler cavity. However, in experimental models the variation has been reduced to the order of 1 percent so that the desired tolerance undoubtedly can be met. Further reduction in the effective asymmetry may, if necessary, be achieved by alternating the orientation of the couplers.

3. *Stray Magnetic Fields*

Stray magnetic fields such as the earth's field must be cancelled quite accurately in order to prevent deflection of the beam. For instance, a transverse field of 0.4 gauss would produce a deflection of several meters over a 10,000 foot length. The field would have to be reduced to $\sim 0.5 \times 10^{-4}$ gauss (for Stage I, 15 Bev), averaged over the entire length, to reduce the deflection to 0.1 cm; the tolerance over any short section of the machine would of course be considerably larger. Such a field cancellation (to 10^{-4} of the earth's field) can readily be effected by some combination of shielding and degaussing. The power requirement for effecting the cancellation entirely by degaussing coils would be small (of the order of one kw), and the regulation requirement (one part in 10^4) would not be prohibitive.

4. *Misalignments*

The problems of machine alignment are probably the most difficult in the whole beam-transport problem. Ideally, the maximum misalignment should be small compared to the accelerator aperture; however, some deviations from straightness will inevitably occur as a result of earth settling, seismic movements, and the limitations of alignment systems. It is necessary either to guide the beam through such misalignments, or somehow to sense and correct the misalignments. Two principles may be considered for guiding the beam: either magnetic steering with transversely uniform fields, or an alternating-gradient strong-focusing system. A third system would consist of some combination of steering and strong focusing. We will summarize the advantages and limitations of each of these systems:

a. Magnetic Steering

Such a system might consist of steering coils or small magnets placed along the machine. The spacing (steering period) would be determined by the short-range alignment of the machine; displacements of the accelerator axis within the steering period should be expected to remain within a few tenths of the hole diameter for a reasonable length of time (i.e., at least a few weeks). A spacing on the order of 100 feet per steering period would appear conservative.

The power requirement, assuming maximum angular misalignments of $\sim 10^{-5}$ radian per steering period, would be very small: of the same order of magnitude as the degaussing power.

The maximum tolerable misalignment would be determined by the first-order dispersion of the beam, i.e., coupling of the energy spread into the transverse coordinates. A maximum linear misalignment of 20 or 30 cm is imposed if the energy spread is about 1 percent.

A considerable complication is introduced in the steering system if multiple beams are to be used (as is presently planned). In a multiple-beam system, beams would be injected at various points along the machine on different machine pulses. In this case, the steering

fields to correct for misalignments would be different for each energy. Hence, it would be necessary either (1) to pulse the steering fields with independently adjustable currents for different beam energies, or (2) to provide means for keeping the maximum misalignment to a small fraction of the accelerator aperture.

This complication has a potentially valuable by-product, however: comparison of the steering currents for the different beams provides an indication of alignment, since the criterion for perfect alignment is that the steering currents in each magnet be the same for all energies. (The steering currents would then be only enough to compensate for locally uncancelled stray magnetic fields.) In fact, even if only a single beam were in use, one could energy-modulate selected pulses (by switching off one or more klystrons) in order to sense and correct misalignments.

b. Strong-Focusing Guide Fields

The possibility of using an alternating-gradient quadrupole system to provide a linear restoring force has several attractive features. First, as has been seen, some focusing is desirable even in an "ideal" machine, to contain the finite transverse momenta introduced in the injector. Second, dc (rather than pulsed) operation of the steering system would be possible even with finite misalignments, the only restriction being that the quadrupoles would have to be more closely spaced in the region immediately downstream from each injector in order to avoid stop bands for the lowest energy. The spacing could be tapered up to about 100 feet per quadrupole pair and thereafter kept constant up to the next injector.

There are at least two effects which tend to limit the maximum usable quadrupole strength. First, chromatic aberration will tend to increase the final transverse phase space through second-order coefficients determined by the energy dependence of the transfer matrix, i.e.:

$$\frac{\partial}{\partial E}\,\frac{\partial(p_x,x)}{\partial(p_{0x},x_0)}$$

That is, in Taylor Series expansions of the transverse coordinates there appear, for example, terms of the form

$$\Delta p_x(p_{0x},\Delta E) = \frac{\partial^2 p_x}{\partial E\,\partial p_{0x}} \cdot p_{0x} \cdot \Delta E \qquad (4)$$

etc., which depend on quadrupole strength. Here p_{0x} is the spread in initial transverse momentum, and ΔE is the spread in accelerating field which gives rise to an energy spread. An upper limit of around 2,000 gauss for the average strength of individual quadrupoles appears to be set in this way.

The second limiting effect is random short-range misalignments which inject transverse momenta of the form $|\delta p_x| \sim |Q\delta x|$, where Q is the quadrupole strength, and δx is the misalignment referred to the local average of the accelerator axis. Rather large local increases in the orbit amplitudes may result if several such transverse impulses happen to reinforce one another. Such quasi-resonances have not been investigated in detail, but there appear to be several possibilities for suppressing them by empirical methods.

The chromatic aberration limitation is found to impose a maximum *systematic* misalignment (e.g., constant curvature) amounting to perhaps 15 or 20 cm in the nominal 10,000-foot length. Thus the alignment tolerance is about the same (within a factor of 2) as in the case of steering fields.

c. Combinations of Steering and Strong Focusing

In a combination system the quadrupoles would be designed primarily for containing the transverse momenta, while the steering (uniform field) magnets would effect the actual guidance of the beam through misalignments. This arrangement would retain the alignment-sensing property of uniform-field steering so long as steering periods are short compared to the wavelengths of transverse oscillations. Chromatic aberration would be small because the quadrupoles would be quite weak. An additional advantage is that the linear dispersion inherent in the uniform-field steering would be largely cancelled out by the orbit cross-overs introduced by the focusing field. Hence the alignment tolerance might be considerably

larger than with either steering or strong-focusing alone.

C. Alignment Principles

As has already been mentioned, the uniform-field steering system with multiple energy (or energy-modulated) beams provides one means of sensing the alignment. In conjunction with suitable beam-position sensing devices and remotely controlled adjustments in the support system, this principle could provide a basis for realignment during operation of the machine.

Other principles which have been proposed include optical methods and stretched-wire techniques.

In order to use an optical system for precision alignment, it would first be necessary to achieve a truly straight line of sight. Transverse density gradients and turbulence of the air must be avoided; for instance, a temperature gradient of 10^{-4} °C/cm at atmospheric pressure would refract the line of sight by ~ 5 cm in 10,000 feet. The line of sight must be enclosed either in a very good thermal shield or in a large vacuum manifold. A maximum error of a few centimeters over a 10,000 foot path implies an angular resolution of $\sim 10^{-5}$ radian or ~ 10 seconds of arc. Optical systems of this quality are probably attainable.

Several different techniques based on stretched wires have been proposed. Such problems as the necessity for careful shielding from air currents and the difficulty of damping out vibrations make these schemes at least as complicated as optical methods; however, the fundamental limitations have not been completely explored, and it is entirely possible that some method of using stretched wires may be able to compete with optical methods.

D. Effects Dependent on Beam Current

1. Space-Charge Forces

As has already been mentioned, the transverse and longitudinal debunching effects become completely negligible at highly relativistic energies. The longitudinal debunching force has, however, a slight effect on energy spread, since electrons ahead of the bunch effectively see a larger accelerating field than those behind the bunch. This effect is roughly estimated as introducing an energy spread of about 1 percent at 100 ma pulse current; however, this could be nearly cancelled by phasing the bunch slightly ahead of the crest of the accelerating wave.

2. Beam Loading

The transient-beam-loading energy spread can be compensated in a number of ways: by modulating the rf pulse, by a combination of early injection and modulation of the current pulse, or by delaying the time of turning on the rf power in several different parts of the machine. The latter scheme seems to be the easiest to apply. Figure 2 illustrates transient beam loading compensation by delaying the timing of three sections consisting of 5, 10, and 20 percent, respectively, of the total machine length. The actual times were chosen empirically. The transient energy spread has been reduced from 10 to <1 percent.

Beam loading will affect the transverse dynamics slightly by the longitudinal field variation effect mentioned in Section III.B.2, but the result is readily shown to be negligible.

3. Beam Blow-Up (Pulse Shortening)

Some effort has been made at Stanford toward understanding the beam blow-up phenomenon. As reported in several laboratories, this phenomenon, also called pulse shortening, is characterized by a sudden disappearance of the beam within individual rf pulses. The disappearance is observed at an increasingly short interval after beam injection as the peak current is increased beyond a certain threshold. For some time it has been suspected that beam blow-up might be caused by a backward-wave (transverse-modulated) oscillation generated in a higher passband by the beam itself. In S-band disk-loaded accelerator guide, the first such passband occurs at about 4,300 Mc/sec. The configuration of this TM_{11}-type mode and its possible radial deflecting properites have been under study at Stanford since 1959.[14] Analysis shows that, at intermediate frequencies, this mode cannot be pure TM in

disk-loaded waveguide and that the transverse electromagnetic force on a synchronous relativistic electron does not in general vanish.

A formulation and numerical solution of this mechanism indeed shows exponential growth of the fields and deflection, provided the group velocity of the deflecting mode is negative and the current is above a certain threshold. For parameters corresponding to the first 10-foot section of the Stanford Mark III accelerator, the exponential growth at 60 ma is calculated to be about a factor of 10^3 per μsec.

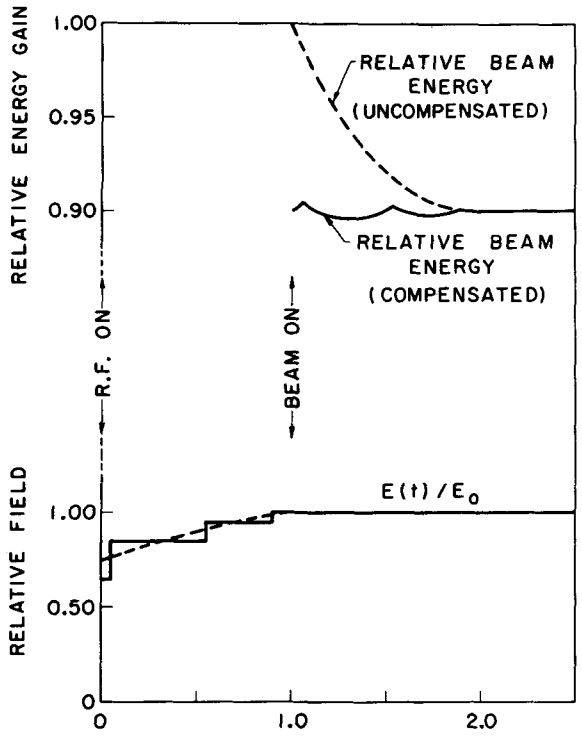

Fig. 2 Beam loading compensation. The lower curves represent effective applied field amplitude: the solid (stepped) curve represents turning on segments of the machine, consisting of 20, 10 and 5 percent of the total, at empirically chosen time delays of 0.05, 0.55, and 0.90 filling time, respectively; the broken curve is a theoretical amplitude which would give exact compensation. The upper curves represent effective energy gain on an expanded scale: the solid curve results from the stepped amplitude function, while the broken line corresponds to a step-function field amplitude turned on at $t=0$. The curves apply to a proposed Project M design (constant group-velocity) with attenuation factor $=0.57$, filling time $=0.87$ μsec, shunt impedance of 0.53 megohm/cm, and 10 percent beam loading (equivalent to $\sim$30 ma, Stage I).

From the point of view of Project M, the situation with respect to beam blow-up is favorable for several reasons. First, as discussed in the next section, the $2\pi/3$ accelerating mode will probably be chosen. In this structure it turns out that the 4,300 Mc mode is very nearly at π-mode cutoff at phase velocity equal to c. This tends to suppress the backward-wave oscillations because (a) the vanishing of the negative group velocity eliminates the feedback mechanism except for short-range group-dispersive effects; and (b) the mode should become essentially pure TM at cutoff, and hence the synchronous deflection of a relativistic electron would nearly vanish.

The other favorable factor is the possible selection of the *constant-gradient* accelerator guide, also discussed in the next section. In such a longitudinally nonuniform structure, as shown in Fig. 3, the variations of the transverse dimensions cause the frequency at which the $v_p=c$ line intercepts the ω-β plot of the respective cavities to change by more than 200 Mc/sec over a 10-foot length. As a result, synchronism would occur only over a much shorter length, and the starting conditions would require much higher currents than expected. Also, the ω-β plots show that the synchronous wave actually is *beyond* π-mode cutoff at the beginning of the section where the deflection interaction would be expected to be strongest because of the smaller longitudinal momentum.[4]

E. Multiple Beam Injection

It has been specified that the accelerator will operate 24 hrs/day for long periods and that multiple beams (up to six) of different energies will be provided on different pulses. For these reasons, a tentative decision has been made to locate only the first injector within the main accelerator tunnel. That is, several of the injection systems will be oriented at an angle with respect to the main accelerator axis.

Several achromatic (nondispersive) magneto-optical inflection systems have been studied on the basis of the following properties:

(1) The first- and second-order geometric optics of a beam of particles passing through the system.

(2) The debunching characteristics.
(3) The alignment tolerances of the various magnetic elements of the system.

Two of the achromatic systems considered which translate a parallel beam to a parallel beam are shown in Figs. 4 and 5. As can be seen from the three characteristic ray diagrams (the monoenergetic transverse ray diagram, the monoenergetic radial ray diagram, and the dispersion ray diagram), three magneto-optical elements are required, two of which must be dispersive. The center element may have dispersion, but this is not a necessary condition.

The path length of any two monoenergetic particles passing through either system will be the same. In fact it can be shown from the work of Streib[5] that this is true for any achromatic system having the initial and final conditions shown in the dispersion ray diagrams of Figs. 4 and 5. However, it is not sufficient for an inflection system to have the same path length for particles of the same energy. If the accelerator bunching characteristics are to be preserved, the path length of all particles should be the same (or nearly so) independent of energy.

The debunching (path-length difference) for particles in the three-identical-bending-magnet system is $(3\alpha - 4 \sin \alpha)\ (\Delta p/p)\rho$, and for the quadrupole system $2(\alpha - \sin \alpha)\ (\Delta p/p)\rho$. Clearly the latter is the preferred system for small α. Because of the opposite sign of the two equations, it is possible to devise achromatic systems having either positive, negative, or zero debunching. One such solution is a combination of the two illustrated systems.

The geometric second-order aberrations have been estimated or calculated for the two sys-

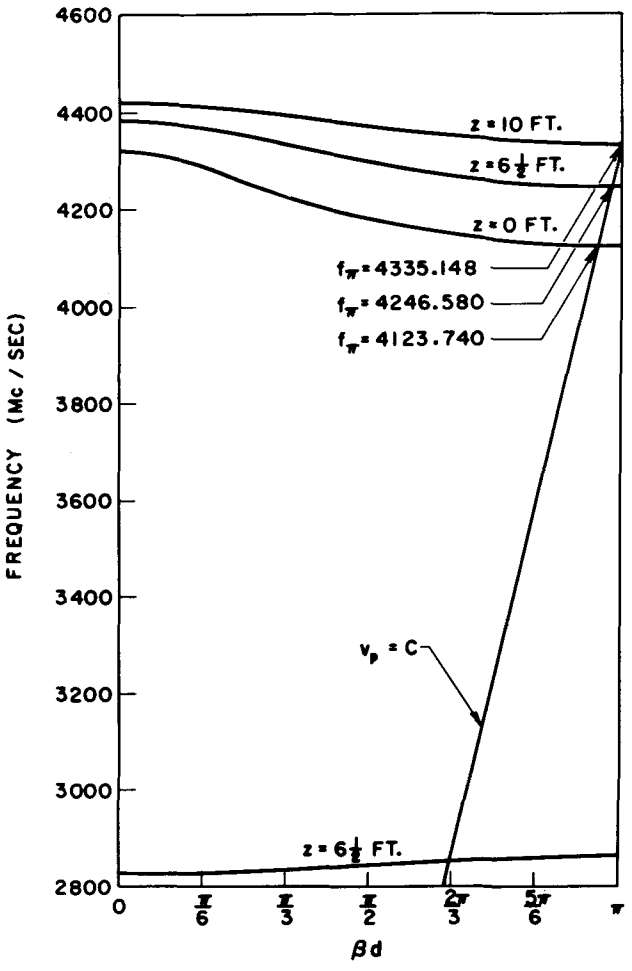

Fig. 3 ω–β diagrams for the fundamental TM_{01} mode at the midpoint of a 10-foot accelerator section, and for the TM_{11} mode at the input, midpoint, and output. Note that the line of $v_p/c = 1$ intersects at three different frequencies.

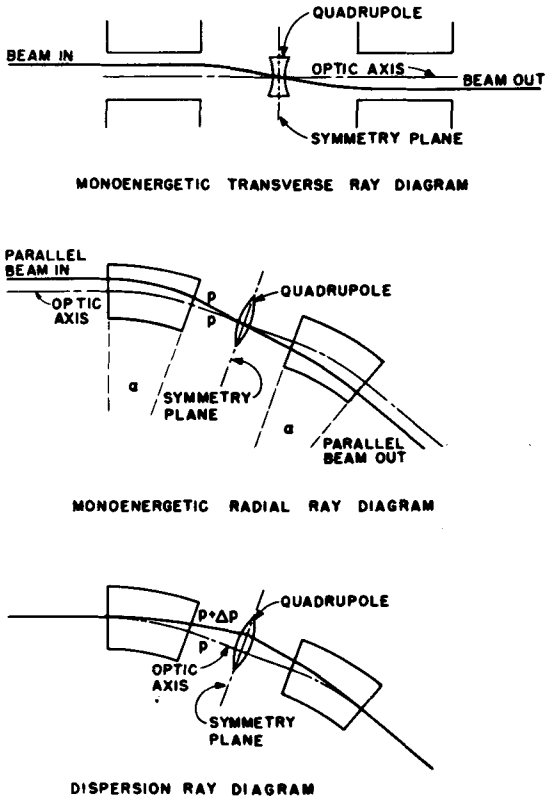

Fig. 4 Achromatic beam inflection system.

tems. If the symmetry about the midplane is preserved, the coefficient of the $(\Delta p/p)^2$ aberration for the exit angle is always zero for systems having an odd number of foci between the entrance and exit.

The dominant second-order term in the exit angle then becomes $CX_0(\Delta p/p)$, where X_0 is the entering beam radius normalized to the bending radius of the inflection system, and C is the order of unity. $CX_0(\Delta p/p)$ is less than 1/1,000 of a radian for typical beam parameters. This combined with the small debunching and practical alignment tolerances make injection at an angle feasible.

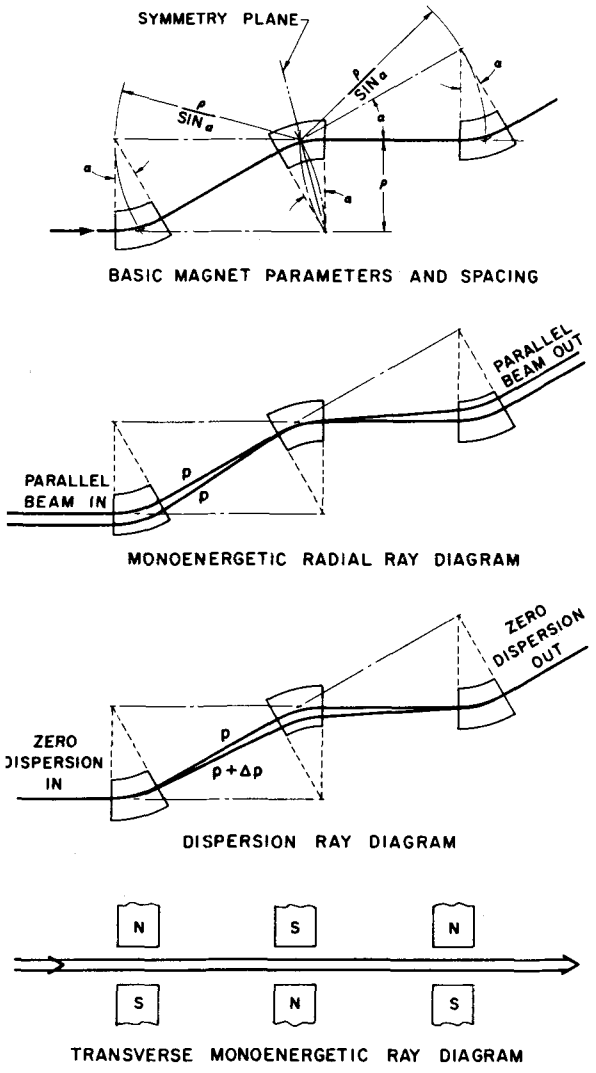

Fig. 5 Achromatic beam inflection system.

IV. ACCELERATOR STRUCTURES

A. INTRODUCTION

The energy of electrons from a linear accelerator with negligible beam-loading is given by

$$V = K\sqrt{P_T L r} \tag{5}$$

where P_T is the total rf power input to the accelerator, L is the total length, r is the shunt impedance per unit length of the accelerator structure, and K is a constant depending upon the net rf attenuation of an individual section. Both K and r depend on the specific design of the accelerator waveguide structure. Assuming that P_T and L are fixed, the choice of a given structure determines the electron energy gain.

In designing an accelerator structure, one is of course interested in not only the total energy gain but also the average electron current and the energy spectrum width. To optimize these three basic parameters, a variety of factors which depend upon the characteristics of the structure must be taken into account. The most important of these factors include the radio-frequency conversion efficiency; the sensitivity to thermal, dimensional and frequency changes; the effect of beam loading; the rf power dissipation per unit length; the group velocity and filling time; the ratio of peak to average electric field strength; and the energy loss when the beam passes through an inactivated section.[6-12]

In the past, an appreciable effort has been devoted to experimental and theoretical investigations of a variety of rf structures for accelerating electrons.[13-16] Rather radical departures from the customary disk-loaded cylindrical guide were examined, such as grid-loaded structures, periodic post or bar structures, and floating-disk structures. Several of these gave promising results, with values of shunt impedance about twice that obtained with the conventional disk-loaded structure; but in every case, when a large improvement in r was obtained, the bandwidth of the structure was excessively high. This resulted in group velocities about 10 times as high as desired, so that recirculation of rf power or extreme lengths between rf feeds would be necessary to obtain maximum utilization of the rf power. The use of feedback would result in undue operational complication, especially in a long, multi-section

accelerator. Several variations of these structures were devised which succeeded in reducing the group velocity to the desired values (in the range of 0.01 c), but these measures caused the shunt impedance to be reduced until no advantage remained; moreover, they resulted in increased fabricational complexity and cost. Considering all pertinent factors, the disk-loaded structure appears superior to all of the other kinds of structures examined to date.

For these reasons, in recent studies we have concentrated on optimizing the design of the disk-loaded cylindrical waveguide. The results so far obtained can be classified into two categories. The first pertain to changes made in the unit accelerator cavity such as the disk spacing d (see Fig. 6), the disk shape (parameters 2a, 2b, ρ), and the disk thickness t. The second pertain to geometrical changes made along an accelerator section to obtain a constant field instead of an exponentially decaying field. Such structures are generally called constant-gradient structures (see Fig. 7).

Scaling of these geometrical properties from one frequency band to another is of course possible. In what follows, we shall limit ourselves to results obtained at $\lambda_0 = 1.5$ cm, which is the wavelength chosen for the 2-mile machine.

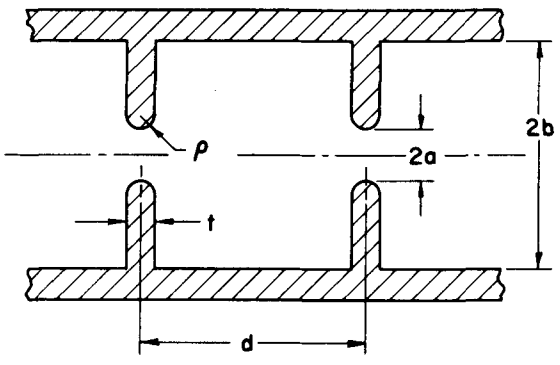

Fig. 6 Two unit cells of the disk-loaded accelerator waveguide.

B. Cavity Dimensions

1. Disk Spacing

The disk spacing d determines the phase shift per cavity. Previous Stanford accelerators have used the $\pi/2$ mode (four disks per wavelength). In accord with theoretical predictions, recent experiments have shown that a 15 percent improvement in shunt impedance can be attained by using the $2\pi/3$ mode (three disks per wavelength). These results are summarized in Fig. 8, where r is the shunt impedance or square of the energy gained per unit length for unit rf power dissipation, δ is the skin depth (taken as 1.23×10^{-4} cm), and the phase velocity v_p is equal to c. The theoretical curves give somewhat higher results than the experiments because they are based on the simple model of a cavity array which neglects the effect of disk aperture. Typical values chosen for further calculation are as follows:

$\pi/2$ *mode*	$2\pi/3$ *mode*
$r = 47$ megohms/meter	$r = 53$ megohms/meter
$Q_0 = 10{,}000$	$Q_0 = 13{,}000$

2. Disk Thickness

The theoretical curves of Fig. 8 also predict that there should be a definite advantage in using thinner disks. Recent studies have confirmed this prediction; the results are shown in

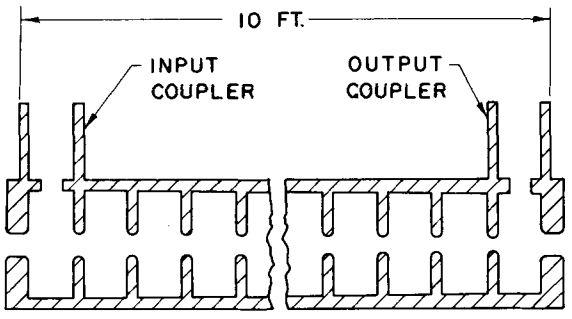

Fig. 7 A sketch of a 10-foot-long constant-gradient accelerator structure, with input and output couplers. Note the decrease in inner and outer diameter in the direction of the beam.

Fig. 9. For reasons explained in the next paragraph, these values were plotted as a function of the normalized group velocity v_g instead of constant 2a. In spite of these results, it has not yet been decided whether disks thinner than about 0.230 inch are suitable in view of mechanical rigidity and electric breakdown considerations. In addition, a narrower heat path might lengthen the time for a given structure to reach thermal equilibrium. High-power tests will be performed in the near future to obtain quantitative information on these points.

3. Disk Diameter and Shape

The disk diameter 2b is fairly narrowly constrained by the operating frequency. However, it is possible, within limits, to vary the disk aperture 2a and the ratio 2a/2b. These determine the group velocity and the attenuation constant α (nepers per unit length). From

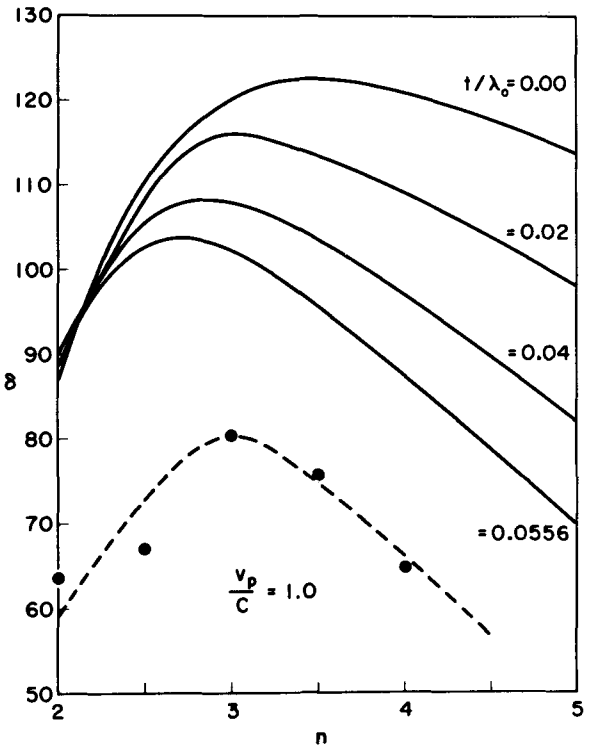

Fig. 8 The quantity $r\delta$ vs n (number of disks per wavelength). The solid curves are computed from a simple model of a cavity array that neglects the effect of disk aperture. The points are averages of experimental values at several disk thicknesses and at a value of $2a = 0.822$ inch. The apertures had unrounded edges.

elementary accelerator theory, the maximum energy gain, at negligible beam current, is attained for $\alpha\ell = 1.26$, where ℓ is the length of the accelerator section. More recent theoretical studies[12] have shown, however, that most of the other design parameters listed above are improved by going to a lower value of $\alpha\ell$. A design for a value of $\alpha\ell = 0.57$ has actually been chosen. This in turn has led to a design of experimental 10-foot sections, operating in the $2\pi/3$ mode with the following parameters:

2a = 0.890 in.	$\ell = 10$ ft
2b = 3.247 in.	$v_g/c = 0.0122$
$t = 0.230$ in.	$Q_0 = 13{,}000$

To reduce the danger of breakdown, the edges of the disk aperture have been rounded. For design purposes, it should be noted that the frequency and the group velocity are rather sensitive to small variations in the aperture contour.[17] The structures described above ($\alpha\ell \cong 0.57$) have actually been built and tested at high power with an electron beam, and most of the predicted advantages have been confirmed.

Further experimental studies to improve rf and thermal properties of individual cavities are presently underway at Stanford. One series of tests is designed to ascertain whether it is possible to obtain improvements in shunt impedance and shorter thermal transients by using wedge-shaped disks. Another series of experiments has been performed[18] to find means of compensating for the field asymmetry caused by the presence of the iris in the coupling

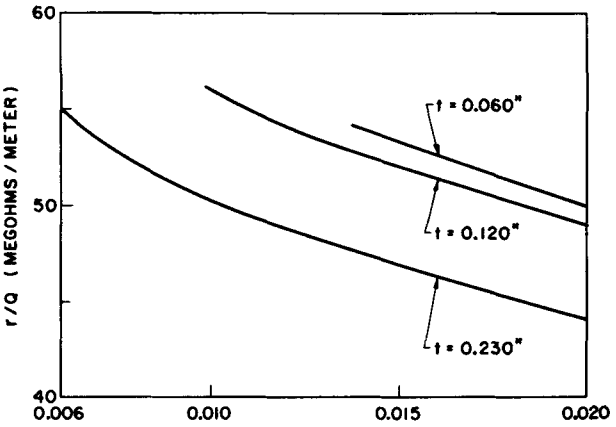

Fig. 9 Values of r/Q vs v_g/c for different disk thicknesses using the $2\pi/3$ mode.

cavities. This asymmetry would cause beam deflection (see Section III.B.2) if it were not cancelled out by such schemes as off-centering the cavity, introducing slugs behind the iris, or making a small hole in the wall opposite the iris.

C. Constant-Gradient Structure

Theoretical studies have been carried out to evaluate the prospective performance of constant-gradient accelerators.[10,11] An outline of the relative merits of such an accelerator as compared to the more common constant-attenuation accelerator is presented in Table 2. The advantages of the constant-gradient structure are clearly shown. Intuitively, it can be seen that in order to obtain such a structure, one must taper down the dimensions of 2a and 2b as a function of length in order to slow down the power flow (i.e., linearly decrease v_g and hyperbolically increase α) so as to compensate for absolute power decay.

Experimental studies have been made to assist in the selection of specific design parameters. Figure 10 shows the exact variation of 2a and 2b as a function of length to achieve an attenuation of ~0.57 nepers. In the absence of a beam, this structure actually gives a slightly increasing gradient as a function of z. Thus, as the current approaches a design value of about 50 to 100 ma peak, beam loading makes the field approach uniformity throughout the 10-foot length. A set of 10-foot sections with these dimensions is presently being fabricated for high-power and electron-beam tests.

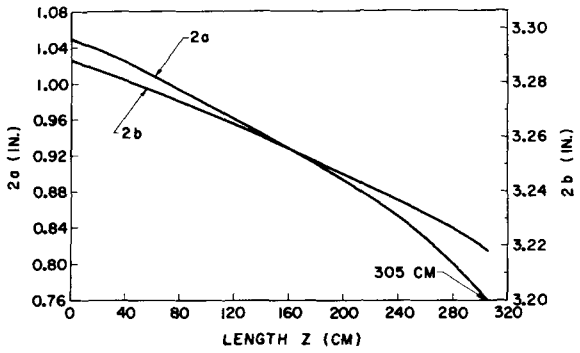

Fig. 10 Values of $2a$ and $2b$ vs distance z for a constant-gradient structure with $\alpha\ell = 0.57$.

TABLE 2

Comparison of constant gradient (c.g.) and constant attenuation (c.a.) accelerator structures at $\alpha\ell = 0.6$

Characteristic	Constant Gradient	Constant Attenuation	Ratio c.g./c.a.
Ratio of peak to average electric field	1.0000	1.3298	0.752
Ratio of rf power loss at input to rf power loss at output of section	1.0000	3.3201	0.301
No-load (zero-current) energy	11.772 Bev	11.600 Bev	1.015
Energy decrease at 50 ma peak current	1.662 Bev	1.708 Bev	0.973
Energy at peak current of 50 ma	10.110 Bev	9.892 Bev	1.022
Maximum beam conversion efficiency	0.724	0.684	1.058
Current at max. efficiency	177.1 ma	169.8 ma	1.043
Normalized group velocity	.0201→.0061	0.0117	1.718→0.521
Filling time	0.872 μsec	0.872 μsec	1.000
Stored energy	731.2 joules	731.2 joules	1.000
Phase shift at 10 ft for frequency change of 0.1 Mc/sec	0.546 rad	0.546 rad	1.000
Relative energy loss for frequency change of 0.1 Mc/sec	0.0357	0.0424	0.842

Assumed parameters

Attenuation per section: 0.6
Total input power: 1,440 Mw
Total length: 9,600 ft (293,000 cm)
No. of sections: 960
Length per section: 10 ft (305 cm)
Angular frequency: 1.79×10^{10} rad/sec
Shunt impedance: 0.47×10^6 ohms/cm
$Q_0 = 13{,}000$

Among the speculative advantages of a constant-gradient structure is the decreased danger of beam blow-up. The advantages in this respect of a nonuniform structure have already been discussed in Section III.D.3.

Before obtaining results from the high-power and beam experiments, we shall retain both uniform and constant-gradient structures as possibilities for the 2-mile machine. However, favorable experience at other laboratories, particularly at the E.N.S. at Orsay, France, with quasi-constant-gradient structures, seems to be very encouraging.

V. METHODS OF ACCELERATOR STRUCTURE FABRICATION

A review of the various possible techniques of fabricating disk-loaded accelerator waveguide indicates that the two preferred methods are electroforming and brazing. Accordingly, a developmental study is being carried out to determine which of these two methods should be used in fabricating the structure for the 2-mile accelerator. By either approach, the disk-loaded waveguide will be made in 10-foot unit sections which include input and output rf couplers.

Approximately 1,000 of these 10-foot unit sections will be connected together in a tunnel to form the required length of interaction structure. The sections will be joined by means of a short length of bellows and heliarc joints.

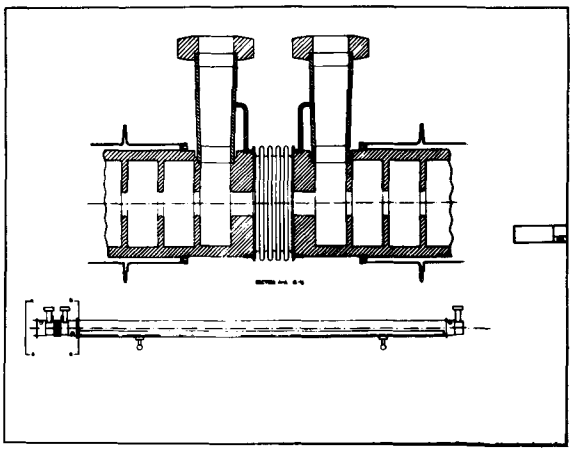

Fig. 11 Sketch of accelerator section showing method of joining sections.

Figure 11 is a representative sketch of a section with its cooling-water jacket. In addition to sheath water cooling, the water jacket will provide the necessary rigidity so that each section need be supported at only two points in the tunnel installation.

Figure 12 shows both the parts for electroforming and brazing as well as the specially designed hollow mill for roughing out the disks. In general, the parts are rough machined for both electroforming and brazing to within 0.010 inch of the finish dimensions and are then stress-relieved before the final machining is carried out.

The electroforming method of fabrication is accomplished by the assembly of a 10-foot array consisting of the copper disks and aluminum spacers shown in the center of Fig. 12. The array is held together by means of a mandrel which passes through its axis. The assembly work is carried out under water to insure that the hydrostatic pressure is equalized, hence reducing the probability of solution leakage. After assembly, the array is processed, and three-eighths of an inch of copper is electroformed over it. After electroforming, the aluminum spacers are etched out with sodium hydroxide. This procedure yields an all-copper disk-loaded waveguide that can be fabricated to very close dimensions.

As a result of a study to determine the most feasible method of fabricating the various parts which go into the 10-foot assemblies for both electroforming and brazing techniques, a boring machine specifically tooled to make these parts has been procured. Included in this study has been an evaluation of the various possible ways of producing the blank accelerator parts that go into the boring machine for final machining. This work indicated that the best approach for electroforming would be to start with forgings of 60-61 aluminum for the spacers, and to hollow-mill the disks from quarter-inch copper strip. For the brazing approach, it appears that the best method is to use individual copper cylinders, and disks which are made in the same manner as those made for electroforming.

A small pilot electroforming set-up has been made for the purpose of evaluating the various factors pertaining to the optimization of the electroforming technique for accelerator sec-

tions. The work with this equipment has reduced the length of time required to deposit ⅜ inch of copper from 6 weeks to slightly over 2 weeks. In the method used, the mandrel is held horizontally, half in and half out of the solution, and is rotated at a speed of approximately 28 rpm. An agate burnisher rides back and forth on the surface of the copper; this results in a continual smoothing of the plated surface. A comparison of the crystal structure of copper electroformed by this technique with that of OFHC copper produced by the usual mill-fabricating procedures shows that the metallurgical properties are excellent. The electroformed copper as it comes from this bath has a surface finish of 6 microinches. After electroforming, it appears that only machining of the ends, to accommodate the coupler, will be necessary. Consideration is now being given to the possibility of fabricating the couplers in sub-assemblies that can be "grown on" to the accelerator section during electroforming.

The study of various brazing possibilities has led to the development of a new type of furnace. The essential features of the furnace are a moving ring burner which is fired by an oxygen-hydrogen flame, and a water-cooled chamber that contains a protective atmosphere for the section to cool in. The unit parts of the accelerator section will be stacked together and aligned horizontally in a V-block, after which the assembly will be suspended as a free pendulum by a long, ⅜-inch-diameter stainless steel tube. In the scale model furnace, which

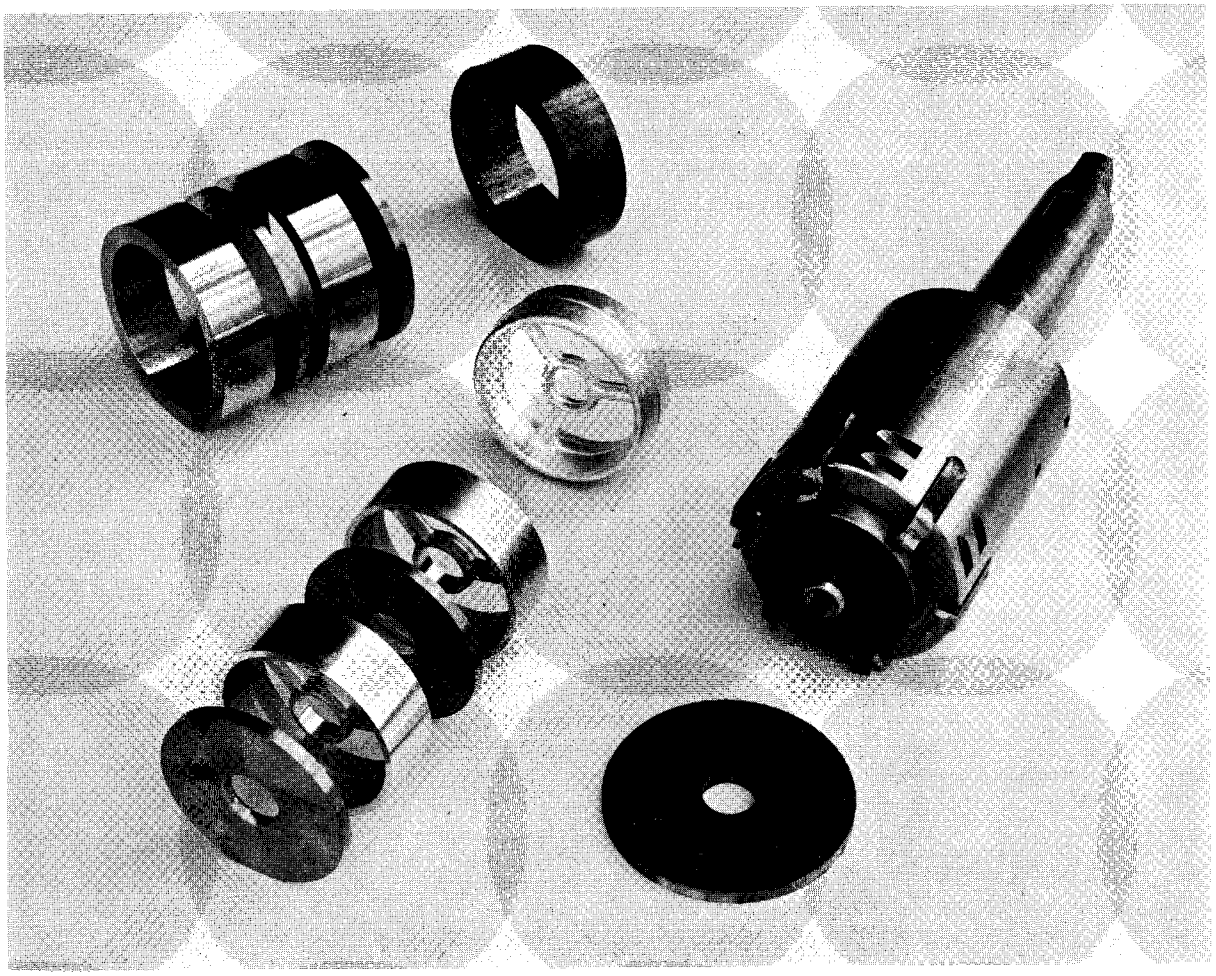

Fig. 12 Accelerator parts and the hollow mill used in roughing out the disks. The copper rings and disks shown in the upper left of the figure are the parts used in the brazing method of accelerator fabrication. The copper disks and aluminum spacers shown in the center of the figure are used in the electroforming method.

will accommodate 24-inch sections, the parts are simply stacked vertically on a base. Figures 13 (A) and (B) show the scale model furnace. After the burner is lighted and the copper under the flame reaches the brazing temperature, the ring burner is moved downward by means of lead screws. The can containing the protective atmosphere follows behind the ring burner at a fixed distance. During the brazing and cooling operations, the

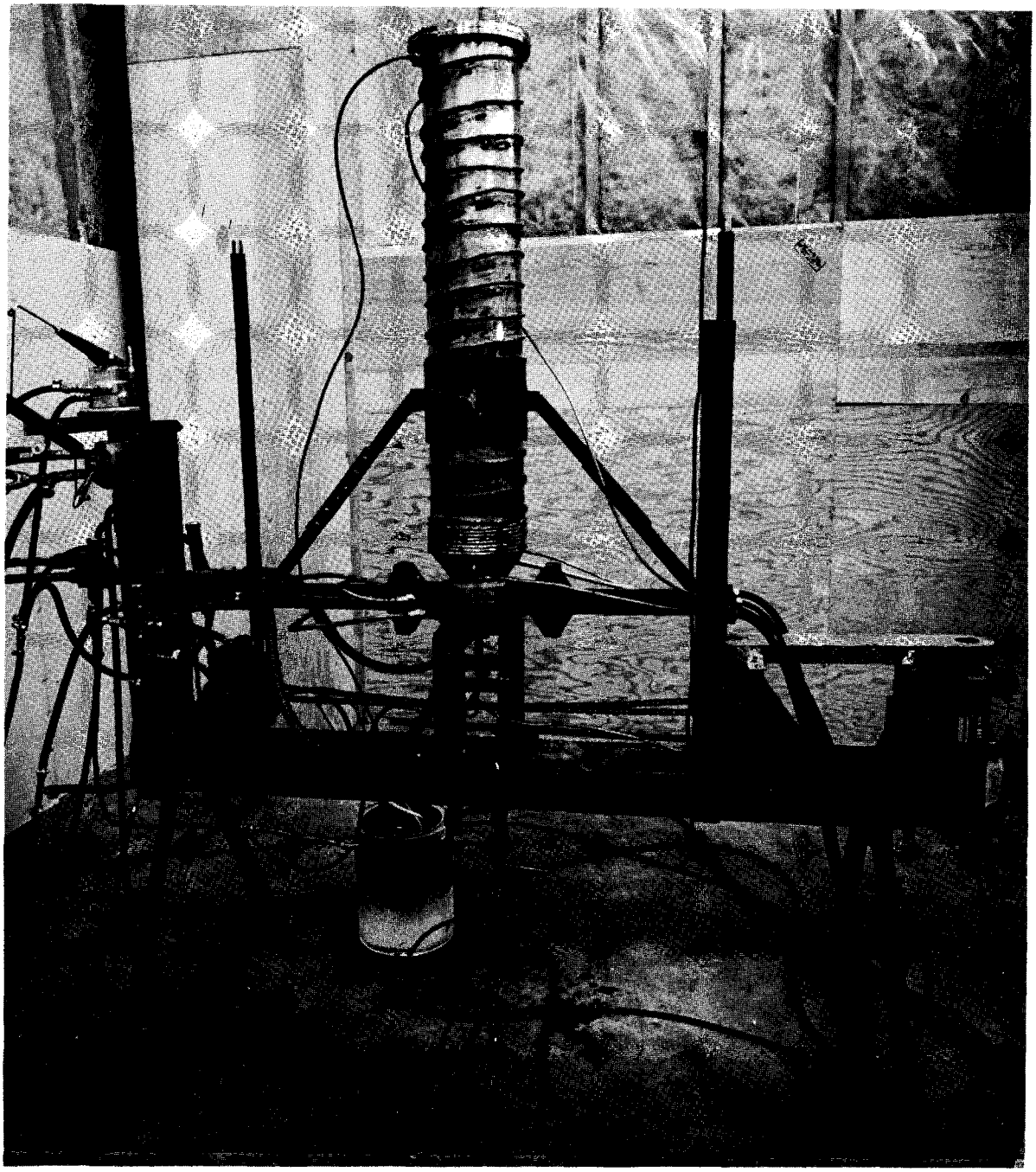

Fig. 13A Scale model of the brazing furnace. The accelerator structure is inside the furnace and cannot be seen in the photograph.

internal surfaces of the accelerator section are protected by means of a flow of pure hydrogen, which is burned off separately from the can. We have successfully used pure hydrogen, and later 90–10 forming gas, in the protective can. Recent work indicates that the 90–10 forming gas will yield highly satisfactory results even for the 10-foot length. Using this technique, it is possible to braze a 16-inch length of accelerator in 4½ minutes, and it will be possible to braze a 10-foot length in about 30 minutes from the time the flame is on until the flame is off. The total cycle time of the furnace will be on the order of 3 hours.

An advantage of this brazing method is the short cycle time, which minimizes creep and crystal growth in the copper. Based on experience with a scale model, the cost of operation and maintenance of this furnace would appear to be substantially less than other types of furnaces of comparable size.

An evaluation has been made of various geometrical configurations for the detail parts that go into making the stacked section for brazing. The two best possibilities were a cup assembly and a disk-cylinder assembly, with the latter now favored on the basis of fabrication convenience. The brazing alloy is placed between the disk and cylinder in the form of a thin washer; at the present time we are using the copper-silver eutectic which melts at 780° C. The flame furnace, because of its capability of minimizing the effects of copper creep, affords the possibility of using some of the copper-gold alloys. Hence it may be possible to eliminate one of the principal

Fig. 13B Close-up of scale model brazing furnace, showing the ring burner moving down over the stacked parts of a short accelerator section.

disadvantages of brazing, namely, that of avoiding the use of silver with its associated poor vapor-pressure qualities.

Disk-loaded waveguide sections having excellent phase-shift characteristics can be made with the use of a tuning technique which consists of slightly deforming the wall of each cavity to compensate for mechanical errors. More specifically, the cavities are made slightly oversized, and the tuning is accomplished by pushing "pea-sized" dimples into the cavity wall. Without the use of this technique, it is unlikely that the brazing method could be made to yield satisfactory sections.

VI. DRIVE AND PHASING

A. General Requirements

A drive system is required to carry low-level radiofrequency power from the master driver at the low-energy end of the accelerator to the rf power amplifiers along the length of the machine. A phasing system is needed initially to adjust the phases of the power amplifiers in proper relationship to the phase of the accelerated electron bunches and subsequently to maintain the correct phase conditions during operation.

The problems of driving and phasing are quite closely related. If the drive system were insensitive to frequency and temperature changes, the phasing requirements could be relaxed since phasing adjustments would be needed only at infrequent intervals (e.g., when a klystron is changed). A less stable drive system might result in the need for such frequent phase adjustments that manual techniques become infeasible and fast-acting automated phasing techniques become essential. The inverse situation, of course, would also apply: the availability of a simple, fast, and inexpensive phasing system would make a less stringent drive system tolerable; a phasing system which is slow or complex to operate would place a premium on using a very stable drive system.

An important decision affecting the designs of the drive and phasing systems of the 2-mile accelerator is that the frequency shall be tunable over a ± 0.1 Mc/sec range, corresponding to correction of a $\pm 2°C$ temperature change in the accelerator structure. Such a temperature change (caused, for example, by a change in the average power level) could in principle be corrected by controlling the cooling-water temperature. Temperature control, however, is much slower than frequency tuning, and cost estimates show that precise control of water temperature is quite expensive in a system of the required magnitude. Fine frequency tuning seems desirable, not only to correct for delays and imperfect compensation in the water cooling system, but also to allow for changes in other parameters such as certain critical pulse shapes. Fast frequency tuning capability is desired to minimize beam energy deviations when parameters such as the pulse repetition rate are changed.

Frequency tuning is accompanied by phase shifts due to dispersion in the drive line components. It is desirable that the energy changes which are the result of frequency tuning should not be confused with energy changes due to frequency-tuning-induced phase shifts in the drive line. This "orthogonality" of control adjustments must be maintained in this case as well as throughout the control system in order that machine tune-up be expeditiously accomplished with minimum ambiguity. To keep this ambiguity within bounds it is necessary either (a) to limit the phase shifts to tolerable levels by choosing drive components having low dispersion characteristics, or (b) to incorporate, at each klystron station along the accelerator, phasing devices having faster responses than the observed frequency tuning effects on beam energy. We have adopted alternative (a) since it appears to be much less complex and less expensive than (b) and since it also results in a drive line which has less temperature sensitivity than a line with greater dispersion. This does not preclude the use of automated phasing systems of advanced design should further studies show that such systems are technically and economically feasible.

As will become clear in the later more detailed discussion of phasing techniques, it may be desirable to have available a stable cw reference signal along the accelerator length for phase comparison purposes. This provides an incentive to design the main drive line for cw opera-

tion and to have it serve both drive and phase-reference functions. Moreover, if rf boosters are used along the drive line (see later discussion) it is much easier to maintain stable phase relationships with cw rather than with pulsed operation.

The designs of the phasing and drive systems, like other parts of the machine, should be compatible with both Stage I (240 klystrons) and Stage II (960 klystrons); it should be possible to make the conversion from the earlier to the later stage with a minimum of equipment obsolescence and minimum loss of experimental time.

Ideally, the characteristics of the drive and phasing systems should allow these necessary functions to be accomplished without interference with the use of the accelerator for research purposes. The relative merits in this respect of the various techniques which have been considered constitute one important basis for evaluation of these methods.

B. Drive Line Considerations

The choice of drive line depends upon the basic requirements discussed above. We will now consider the question of drive line phase shifts. Among the factors potentially contributing to phase shift are: frequency dispersion and temperature variations in the drive line (including the waveguide between the klystrons and the accelerator), changing operating conditions in the drive system rf amplifiers and associated electronic circuitry, and possible differential ground displacements along the 2-mile length.

The *relative* phase shift between the rf wave in the drive line and the electron bunches is given by[19]

$$\frac{\delta\Phi}{\Phi} = \frac{\delta\Phi_e - \delta\Phi_w}{\Phi_e} = \left(\frac{\delta z}{z}\right)_e - \frac{c}{v}\left(\frac{\delta z}{z}\right)_w + \left(1 - \frac{c}{v}\right)\frac{\delta\omega}{\omega} + \frac{c}{v}\frac{\delta v}{v} \qquad (6)$$

where subscripts w and e refer to rf wave and electron variations respectively, v is the phase velocity of the rf wave in the drive line, and c is the velocity of light. As can be seen, the total variation is the sum of length variations ($\delta z/z$ terms), wavelength variations ($\delta\omega/\omega$ term), and dispersion ($\delta v/v$ term).

On a short-term basis, only the last two terms of Eq. (6) (which have frequency dependence) need to be considered. The change in beam energy varies as the square of the phase shift (for small angles) whether the phase shift occurs in the accelerator sections ($\delta\theta$) or in the drive line ($\delta\Phi$). To assure that frequency and phase adjustments remain essentially orthogonal, it is necessary that

$$(\delta\Phi)_\omega^2 \ll (\delta\theta)_\omega^2 \qquad (7)$$

The phase shift in each accelerator section caused by a frequency change $\delta\omega$ is

$$(\delta\theta)_\omega \cong 360\,\frac{c}{v_g}\,\frac{\ell}{\lambda}\,\frac{\delta\omega}{\omega} \quad \text{(degrees)} \qquad (8)$$

where ℓ is the length of the accelerator section, v_g is the group velocity in the section, and λ is the wavelength. For the chosen parameters of the 2-mile accelerator ($c/v_g \cong 81.3$, $\ell/\lambda \cong 29$), Eq. (8) becomes $(\delta\theta)_\omega = 8.5\times10^5\ \delta\omega/\omega$ degrees. For example, a 0.1 Mc/sec change in frequency (at 2,856 Mc/sec) results in a 30-degree phase shift of the rf wave by the time it reaches the end of each accelerator section. Satisfaction of the condition of Eq. (7) requires that $(\delta\Phi)_\omega \ll 8.5\times10^5\ \delta\omega/\omega$ degrees or $(\delta\Phi/\Phi)_\omega \ll 0.08\ \delta\omega/\omega$ for a length of 10,000 feet and a frequency of 2,856 Mc/sec.

The above quantitative requirement of phase stability in the presence of frequency changes could conceivably be satisfied by the use of either hollow waveguide or coaxial transmission lines in the drive system.

1. *Hollow Waveguide Drive Line*

The hollow waveguide line offers the advantage of not requiring a center conductor with the attending support and cooling problems. However, waveguides have velocity dispersion due to the fact that guide wavelength changes more rapidly with frequency than free-space wavelength. The dispersion can be reduced to any desired degree by increasing the physical dimensions of the waveguide, but the problem of higher mode propagation then arises. Provision of means of suppressing higher order modes is probably

essential, primarily to prevent random or variable coupling of modes with attendant power variation and phase shift in the desired mode. From waveguide theory, it can be shown that the ratio of free-space wavelength λ_0 to the cutoff wavelength λ_c is given by[19]

$$\frac{\lambda_0}{\lambda_c} = \left[1 - \left(\frac{\left|\frac{\delta\omega}{\omega}\right|}{\left|\frac{\delta\omega}{\omega}\right| + \left|\frac{\delta\Phi}{\Phi}\right|}\right)^2\right]^{1/2} \qquad (9)$$

where $\delta\Phi/\Phi$ is the fractional phase shift of the waveguide wave with respect to a free-space wave of the same frequency caused by the fractional frequency change $\delta\omega/\omega$. According to arguments given in the previous paragraph, it is desirable that $\delta\Phi/\Phi \ll 0.08\ \delta\omega/\omega$; in this example, suppose that $\delta\Phi/\Phi = 0.02\ \delta\omega/\omega$. Then Eq. (4) becomes

$$\frac{\lambda_0}{\lambda_c} = \left[1 - \left(\frac{1}{1.02}\right)^2\right]^{1/2} = 0.197$$

and thus, for $\lambda_0 = 10.5$ cm, $\lambda_c = 53.3$ cm. The phase velocity of the wave in a structure having such characteristics is 1.02 times the velocity of light.

The dimensions of waveguide having a cutoff wavelength of 53.3 cm depend upon the shape of the guide and the propagating mode. Three possible cases are summarized in Table 3.

2. Coaxial Drive Line

Coaxial structures are attractive for the drive line application since they are far less dispersive than hollow waveguide.[20] Commercial coaxial lines are available for which $v/c \cong 0.996$ and $\delta v/v < 10^{-8}$ for $\delta\omega/\omega = 1/30{,}000$. Such lines have an attenuation of $\sim$1 db/100 feet and will therefore require rf boosters along the 10,000-foot length.

During short-term tuning procedures the first two (length variation) terms in Eq. (6) can be neglected, and this equation becomes

$$\left(\frac{\delta\Phi}{\Phi}\right)_\omega = \left(1 - \frac{c}{v}\right)\frac{\delta\omega}{\omega} + \frac{c}{v}\frac{\delta v}{v} \qquad (10)$$

For a coaxial line having the characteristics given above, Eq. (10) gives $(\delta\Phi/\Phi)_\omega \cong 10^{-7}$ which is an order of magnitude better phase stability than required according to the considerations described above.

3. Effect of Temperature Variations

In studying temperature effects we again make use of Eq. (6). In the coaxial line case

TABLE 3

Waveguide Dimensions and Theoretical Attenuations for Three Modes at λ_0 = 10.5 cm, λ_c = 53.3 cm

Waveguide shape	Mode	Electric field configuration	Cutoff wavelength	Waveguide dimensions for λ_c = 53.3 cm	Attenuation in 10,000 feet
Rectangular	TE_{10}	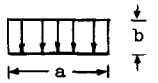	$\lambda_c = 2a$	a = 26.6 cm b = 13.3 cm	7.8 db
Circular	TE_{11}	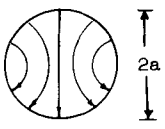	$\lambda_c = 1.706\ (2a)$	2a = 31.2 cm	2.9 db
Circular	TE_{01}	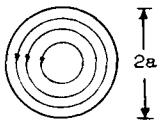	$\lambda_c = 0.820\ (2a)$	2a = 65 cm	0.12 db

the last two terms are negligible, and only the length variation terms need be considered. In the case of waveguides, the last term containing $\delta v/v$ is significant since the phase velocity is a function of the guide cutoff wavelength λ_c which varies with temperature. In this case, it is preferable to write Eq. (6) in the form[19]

$$\frac{\delta\Phi}{\Phi} = \left(\frac{\delta z}{z}\right)_e - \frac{c}{v}\left(\frac{\delta z}{z}\right)_w + \left(\frac{v}{c} - 1\right)\frac{\delta\lambda_0}{\lambda_0} - \frac{v}{c}\left[1 - \left(\frac{c}{v}\right)^2\right]\frac{\delta\lambda_c}{\lambda_c} \tag{11}$$

Many different cases of temperature variation can be studied using Eqs. (6) and (11). For example, we have considered elsewhere[19,20] the cases where the temperatures of both accelerator structure and drive line are assumed to vary, both with and without frequency tracking of the accelerator temperature. For simplicity, in this report attention will be confined to the case where the temperature of the accelerator structure and the operating frequency are held constant while the drive line temperature is assumed to vary. In the coaxial line case with $c/v \cong 1$, Eq. (6) then becomes

$$\left(\frac{\delta\Phi}{\Phi}\right)_{\text{coax}} = -\left(\frac{\delta z}{z}\right)_w = -g_w\,(\delta T)_w \tag{12}$$

where g_w is the temperature coefficient of expansion of the drive line material. For copper structures, $g_w = 1.6\times10^{-5}/^\circ$ C, in which case

$$\left(\frac{\delta\Phi}{\Phi}\right)_{\text{coax}} = -1.6\times10^{-5}\,(\delta T)_w \tag{13}$$

The decrease in accelerator energy which results from this cumulative phase shift in the drive line (varying linearly from 0 at the low-energy end to $\delta\Phi$ at the high-energy end of the accelerator) is given by

$$\left(\frac{\delta V}{V}\right)_{\delta\Phi} = \frac{\sin\delta\Phi}{\delta\Phi} - 1 \cong -\frac{(\delta\Phi)^2}{6} \tag{14}$$

Thus, to keep the energy within 0.5 percent of maximum without re-phasing, it is necessary that the total drive line phase shift be held to ~10 degrees, which in turn [from Eq. (13)] requires that the temperature be held within 0.06°C. With similar reasoning for the waveguide case, Eq. (11) becomes

$$\left(\frac{\delta\Phi}{\Phi}\right)_{\text{w.g.}} = -\frac{v}{c}\,g_w\,(\delta T)_w \tag{15}$$

Thus, for v/c close to unity only slightly closer temperature tolerance is required for waveguides than required for the coaxial line.

In the above examples, it has been assumed that the drive line is free to slide as its temperature varies. This assumption clearly leads to temperature tolerances which would be extremely difficult and expensive to maintain. Two alternatives appear to offer means of relaxing the tolerances:

(a) The drive line can be anchored periodically to ground with expansion and contraction of the line taken care of by means of bellows or sliding joints.

(b) The drive line (without bellows) can be rigidly tied to the accelerator feed points, thereby governing the expansion of the accelerator sections (each 10-foot accelerator section is equipped with a bellows at its output end).

In alternate (b) absolute axial motion of the two systems is permitted but relative motion is prohibited. Since the motion is governed by the drive line, the condition is

$$\left(\frac{\delta z}{z}\right)_e = \left(\frac{\delta z}{z}\right)_w = g_w\,(\delta T)_w \tag{16}$$

Substituting Eq. (16) in Eqs. (6) and (11) (with fixed frequency) gives:

$$\left(\frac{\delta\Phi}{\Phi}\right)_{\text{coax}} = \left(1 - \frac{c}{v}\right) g_w\,(\delta T)_w \tag{17}$$

$$\left(\frac{\delta\Phi}{\Phi}\right)_{\text{w.g.}} = \left(1 - \frac{v}{c}\right) g_w\,(\delta T)_w \tag{18}$$

For coaxial line with $|(1-c/v)| \cong 4\times10^{-3}$ and for waveguide with $|(1-v/c)| \cong 2\times10^{-2}$ the temperature tolerances of the drive lines to limit $\delta\Phi/\Phi$ to 10^{-6} are

$$(\delta T)_{w(\text{coax})} = 15.6^\circ\text{C} \tag{19}$$

$$(\delta T)_{w(\text{w.g.})} = 3.1^\circ\text{C} \tag{20}$$

Alternate (b) has the disadvantage that the drive line must be in the accelerator tunnel

where the radiation environment makes servicing difficult and may result in phase shifts.[21] Alternate (a) permits the drive line to be located in the klystron gallery but introduces questions concerning relative ground motion between the tunnel and gallery. The above analysis remains valid provided that no shearing ground motions occur between these two structures. The advantages of having the drive line in the klystron gallery are enough to outweigh the concerns with relative ground motion. Moreover, even if the ground motion is sufficient to require re-phasing it is expected to be slow enough that any of the phasing techniques under consideration can readily accomodate this eventuality.

4. Drive Line Design

The final choice of drive line for the 2-mile accelerator has not yet been made. However, a schematic layout of a proposed drive system using a coaxial main drive line in the klystron gallery is shown in Fig. 14. Since the attenuation of the proposed coaxial line is ~1 db/100 feet it is necessary to boost the power periodically along the accelerator length. (The drive system with a waveguide main drive line would be similar except that cw boosters would not be required.)

Five cw *main booster* stations are provided along the main drive line. Two cw klystron amplifiers, each capable of 30 watts output, are located at each main booster station. Only one of these tubes is in service at one time; the spare tube can be placed into operation by means of a suitable rf switch. Each main booster provides cw power for six 320-foot accelerator sectors. Because of the low power-handling capacity of the coaxial line (and because the power is cw), the rf power coupled from the main drive line to provide drive for each sector must also be boosted. This function is performed by 30 pulsed *sub-boosters*, one for each sector. The rf power from the sub-boosters is delivered to the final klystron amplifiers through either coaxial line or waveguide. The use of waveguide may be permissible since the phase shifts incurred in the various sector drive lines are not cumulative over 10,000 feet as in the main drive line. Isolators are provided before the sub-boosters and the final klystron amplifiers to prevent instabilities due to possible power reflections.

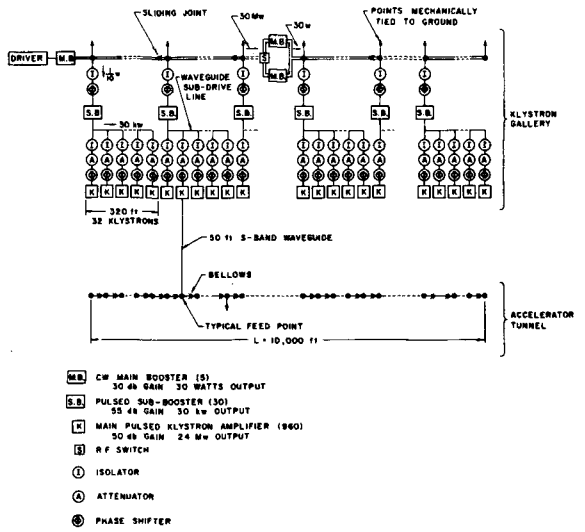

Fig. 14 Tentative drive system for 2-mile accelerator (Stage II).

C. Phasing

The phasing system must be designed to provide methods and equipment with which the rf sources along the accelerator can be phased to produce electron beams of maximum energy and minimum energy spectrum. It is desirable that the necessary phasing procedures be accomplished with minimum interference with research use of the machine.

A number of phasing schemes have been studied and will be discussed below. On the 2-mile machine, it may turn out that more than one method is needed. One method may be preferable for initial phasing, another for subsequent re-phasing; one method may be preferable for phasing individual klystrons, another for phasing entire sectors; etc.

1. Phasing Accuracy

The accuracy to which the rf sources must be phased depends upon how closely one expects the output energy to approach the ultimate performance level (perfect phasing). The total electron energy V_T is the sum of the individual contributions of the N accelerator sections, i.e.,

$$V_T = \sum_0^N V_n \cos \theta_n \qquad (21)$$

where V_n is the maximum possible energy gain (for given rf power input), and θ_n is the phasing error in section n. For small values of θ_n and equal values of V per section, Eq. (21) may be written

$$V_T \cong VN\left(1 - \tfrac{1}{2}\,\overline{\theta^2}\right) \qquad (22)$$

where $\overline{\theta^2}$ is the average value of θ_n^2. Thus, if one wishes the accelerator energy to attain 99.5 percent of its maximum value, it is necessary that $\theta^2 = 0.01$. This means that the phasing devices must accomplish their function within a standard deviation of 0.1 radian or approximately 5 degrees. This is the phasing tolerance that has tentatively been adopted for the 2-mile accelerator.

With perfect phasing and electrons bunched with uniform distribution within an angular spread of α degrees, the energy spectrum width expressed as a fraction of maximum energy is

$$\frac{\Delta V_T}{V_{T_{(\max)}}} = 1 - \cos\frac{\alpha}{2} \cong \frac{\alpha^2}{8} \qquad (23)$$

For example, to obtain a spectrum width of 0.5 percent, $\alpha = 0.2$ radians $\cong 12$ degrees. Since we are trying to limit the spectrum width to 0.5 percent and since bunching angle is only one of several causes of spectrum broadening, we are endeavoring to limit the bunching spread to 5 degrees. In case of imperfect phasing, the spectrum width increases to

$$\frac{\Delta V_T}{V_{T_{(\max)}}} = 1 - \frac{\cos(\alpha/2)}{\left[1 + \left(\frac{\sum V_n \sin\theta_n}{\sum V_n \cos\theta_n}\right)^2\right]^{1/2}} + \frac{\sin(\alpha/2)}{\left[1 + \left(\frac{\sum V_n \cos\theta_n}{\sum V_n \sin\theta_n}\right)^2\right]^{1/2}} \qquad (24)$$

for

$$\tan\frac{\alpha}{2} \geq \frac{\sum V_n \sin\theta_n}{\sum V_n \cos\theta_n}$$

However, if $\Sigma V_n \sin\theta_n = 0$, i.e., if, in the practical case, the algebraic sum of the phasing errors in the accelerator sections equals zero, then the spectrum width given by Eq. (24) reduces to $1 - \cos(\alpha/2)$. This is an important result since it means that the percentage spectrum width can be rather easily maintained equal to that obtained with perfect phasing. If the phasing errors do not add algebraically to zero, they can be made to do so simply by adjusting the phase of one or more klystrons or accelerator sectors until minimum spectrum width is obtained. Thus, the required accuracy of phasing the individual sources is determined *not* by spectrum width considerations but by the allowed deviation from the maximum possible beam energy [Eq. (22)].

The considerations of the last paragraph refer primarily to the phasing errors *per se*, i.e., the tolerances which the individual phasing devices are capable of achieving. To study the effects on spectrum width of drive-line phase deviations, it is helpful to write Eq. (24) in a simpler form, valid for small α, small $\theta(n)$, and for $\alpha/2 \geq \sum\theta_n/N$. This equation then becomes

$$\frac{\Delta V_T}{V_{T_{(\max)}}} \cong \frac{1}{2}\left[\frac{\alpha}{2} + \frac{\sum\theta_n}{N}\right]^2 \qquad (25)$$

The quantity $\sum\theta_n$ is the *net* phasing error, i.e., the algebraic sum of the individual section phasing errors. As an example, suppose that dispersion or temperature effects cause the drive line propagation characteristics to change so that the section phasing errors increase linearly from 0 at the low-energy end to α at the high-energy end of the accelerator. In this case, all the phasing errors would be of the same sign, and the average phasing error $\sum\theta_n/N$ would be $\alpha/2$. Thus, from Eq. (25) the spectrum width would be $\alpha^2/2$, i.e., four times as broad as the minimum width, $\alpha^2/8$. However, as pointed out above, the spectrum could be restored to its minimum width by adjusting the sector phases to cause $\sum\theta_n = 0$.

2. *Phasing Methods*

A number of phasing techniques which have potential application to the 2-mile accelerator will now be discussed. These methods are as follows:

(a) Maximization of electron beam energy.
(b) Direct rf phase comparison.
(c) Interaction between electron beam and rf wave.
   Resistive loading.
   Reactive loading.
   Beam induction.

a. Beam Energy Maximization

This method is based upon observation of the beam energy as the rf power from a particular rf source is perturbed in amplitude (e.g., off-on) or in phase. When the phase of the rf source is correctly adjusted, the beam energy gain will be maximum; equivalently, when the amplitude of the source power is perturbed, a maximum change in output beam energy will result when the phase is correct. It would probably be desirable to perturb the klystron at a frequency that is unrelated to the power line frequency or pulse repetition rate in order to make separation of the wanted effect from the system "noise" more readily achievable.

Where a single klystron is being perturbed while the output beam from the entire machine is observed, it might appear that the effect being measured would have a magnitude of only $1/N$ (or $2/N$ for the phase-shift scheme) of the total signal, where N is the number of klystrons in operation. This assumption is true in terms of beam energy; however, the quantity being primarily observed is *not* the energy but the analyzed beam current. For a sharp energy spectrum, the percentage change in analyzed current can be 100 to several thousand times the percentage change in beam energy depending upon the width and shape of the spectrum curve.[22]

In comparison to other methods of phasing, this method has the advantages that it requires no additional microwave circuitry or vacuum components along the accelerator length and that it is feasible at either high or low currents. Further work is necessary to determine whether this method is sufficiently sensitive for phasing individual klystrons with respect to the entire machine; however, it seems certain that it will be useful in adjusting or checking the phase of individual sectors.

b. Direct rf Phase Comparison

In this method, all the klystrons of a 320-foot sector are phased with respect to a klystron in the center of the sector by comparing phases of the rf waves in the feed lines just before they enter the accelerator. Starting from the center klystron, the phases of klystrons on each side are set using suitable phase detectors. The desired relative phase of the adjacent feeds can be determined from the known axial separation of the feeds. Similar phase comparisons and adjustments proceed in both directions until all the klystrons in the sector are phased. With standard techniques, it should be possible to adjust each individual klystron to an accuracy of 1 percent of a wavelength or better. The errors with respect to the phase of the electron bunches should increase in a "random walk" manner. Thus, if the error of a single adjustment is θ, the expected phase error of the n'th section from the center would be $n^{1/2}\ \theta$.

From the above probable phase error accumulation, it can be shown that the average energy per section of the sector is [15]

$$V_{av} = V_0 \left[1 - \frac{\theta^2}{4} n\right] \tag{26}$$

where V_0 is the energy gained in the section for perfect phasing, and $2n$ is the number of sections in the sector. For example, with $\theta = .05$ radian and $2n = 32$, we obtain

$$V_{av} = 0.99\ V_0 \tag{27}$$

i.e., the average energy loss from imperfect phasing is 1 percent of the total energy.

The direct phase comparison method might be useful in phasing all the klystrons of each sector. Then, the energy maximization technique could presumably be used to phase the sectors with respect to the entire machine.

c. Interaction Between Electron Beam and rf Wave Resistive Beam Loading[23]

When an electron beam passes through an accelerator section filled with rf energy, a fraction of this energy is delivered to the beam, and the rf power level in the section decreases. When the section is correctly phased, the power reduction is maximum. If a phase error θ exists between the electron bunches and the wave at entry, the steady-state rf power flow at the exit ($z = \ell$) is[24]

$$P(\ell) = P_0 e^{-2\alpha\ell} + \frac{i^2 r}{2\alpha}\left(1 - e^{-\alpha\ell}\right)^2 - 2i\left(\frac{P_0 r}{2\alpha}\right)^{1/2}\left(1 - e^{-\alpha\ell}\right)e^{-\alpha\ell}\cos\ \theta \tag{28}$$

where P_0 is the input rf power, ℓ is the length of accelerator section, α is the rf attenuation coefficient (nepers/unit length), i is the peak beam current, and r is the shunt impedance per unit length.

$$\sigma = \frac{(dP/d\theta)}{P_0 e^{-2\alpha\ell}} = 2i\left(\frac{r}{2\alpha P_0}\right)^{1/2}\left(1 - e^{-\alpha\ell}\right) e^{\alpha\ell} \sin\theta \tag{29}$$

Thus, for small phasing errors, the observed change in output rf power is proportional to the error. For example, suppose that $i=10$ ma, $P_0=24$ Mw, $r=0.53\times10^6$ ohms/cm, $\ell=305$ cm, and $\alpha\ell=0.57$. For these assumed parameters, we obtain $\sigma\cong7\times10^{-4}$ parts/degree. From inspection of Eq. (29) it is seen that the sensitivity can be increased by increasing i or decreasing P_0, but there are practical limits to this procedure. The low sensitivity of this method is its major disadvantage.

Reactive beam loading

This method is based on the fact that the passing electron beam causes a phase shift in the output rf power from an accelerator section unless the section is correctly phased (this method is ambiguous in that no phase shift occurs when there is a phase error of 180 degrees; however, the latter case can be detected from the fact that the output rf power exceeds its no-load value).

Reactive beam loading can be explained as follows.[25] There are two electric waves present in the accelerator section. The amplitude of the impressed rf wave from the klystron power source will be designated as E_w, while that excited by the electron beam will be called E_e. The impressed wave E_w decays with distance ($E_w=E_0e^{-\alpha z}$), while the induced wave E_e grows with distance [$E_e=ir\ (1-e^{-\alpha z})$]. When the phasing is correct, these two waves will be oriented as shown in Fig. 15a. When the phasing is incorrect, the orientation will be as shown in Fig. 15b. The resultant rf wave is given by

$$|E_R|^2 = E_e^2 + E_w^2 - 2E_eE_w\cos\theta \tag{30}$$

The rate of change of the phase angle Φ of the resultant wave with respect to the phase angle between the electron bunches and the rf wave θ at the output of the accelerator section is[25]

$$\lim_{\theta\to0}\left|\frac{d\Phi}{d\theta}\right| = \frac{1}{\frac{E_w}{E_e} - 1} \tag{31}$$

where

$$\frac{E_w}{E_e} = \left(\frac{2\alpha P_0}{i^2 r}\right)^{1/2}\frac{1}{e^{\alpha\ell} - 1}$$

The sensitivity of this method also increases with increasing beam current i and decreasing rf power input P_0. For the same values of the parameters assumed in the resistive beam loading example, we obtain $|d\Phi/d\theta|\to0.02$. Thus, in this example, to adjust the phase angle θ to an accuracy of 5 degrees it is necessary to measure the output phase angle to an accuracy of 0.1 degrees.

A block diagram of the rf instrumentation needed for this method is shown in Fig. 16. The rf power from klystron K_n is transmitted through a section of the accelerator, and the

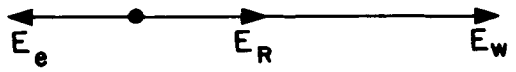

ORIENTATION OF FIELD VECTORS WHEN PHASING IS CORRECT

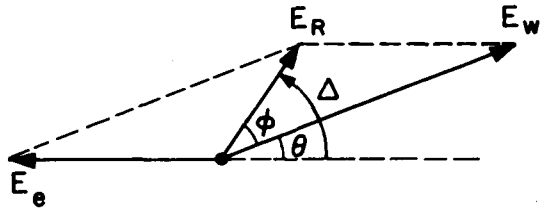

ORIENTATION OF FIELD VECTORS WHEN PHASING IS INCORRECT

Fig. 15 Vector diagram illustrating principle of phasing accelerator section by reactance loading method.

phase of the output wave from the coupler is compared with the phase of the wave before it enters the section. With the electron beam off, a null of the phase detector is obtained by adjusting phase shifter A. When the beam is turned on, a change in the output phase results unless the phasing between the electrons and the wave is correct. Correct phasing can thus be obtained by adjusting phase shifter B to re-establish the null.

Beam induction

In this method, the electron beam passing through the accelerator section being phased (in the absence of an externally impressed field) sets up a wave which provides a phasing reference. This reference wave is 180 degrees out of phase with respect to the optimum phase adjustment of the wave from the external power source. The measurements in this case are made with the klystron alternately off and on (or shifted in time) using rf circuitry similar to that shown in Fig. 16. However, a signal from the drive line is used as an input to the phase detector instead of a sample of the accelerator input power as shown in the figure.

The beam induction method has much better sensitivity than the reactive and resistive beam loading methods, especially at low beam current levels. Referring to Fig. 15 this sensitivity is seen to be

$$\frac{d\Delta}{d\theta} = \frac{d\Phi}{d\theta} + 1 = \frac{\frac{E_w}{E_e}}{\frac{E_w}{E_e} - 1} \qquad (32)$$

Thus, the sensitivity is E_w/E_e times as high as that of the reactive beam loading method [Eq. (31)]. For the parameters used in our previous examples this ratio of improvement is $\sim$50.

To conclude, several phasing techniques are still being evaluated. The energy perturbation technique is probably the least complex and least costly of all the methods under consideration; it will undoubtedly be useful in phasing sectors but whether its sensitivity is sufficient to permit phasing individual klystrons requires further investigation. The beam induction technique is the most sensitive and generally preferable of all the methods involving interaction between the electron beam and the rf wave.

VII. KLYSTRONS

A. Introduction

In this section we describe some of the development work done at Stanford on the klystron power amplifiers for the 2-mile accelerator. Tube types other than klystrons have been evaluated as possible radio-frequency power sources for this accelerator application (specifically the Amplitron tube manufactured by Raytheon Company), but combined tube and system requirements presently dictate the choice of klystrons.

Because of the large complement of tubes, the costs associated with klystron replacement and repair will be substantial. With 240 klystrons and an assumed average operating life of 2,000 hours per tube, the failure rate would be about 3 tubes each day of operation. Thus the present klystron development program has had as one of its objectives the design of a tube with long life, reliability, and ease of fabrication and maintenance, in addition to desirable performance characteristics. These and other factors have resulted in the design of a tube (called the M klystron) that is considerably different from the tubes now used on the Stanford Mark III accelerator.

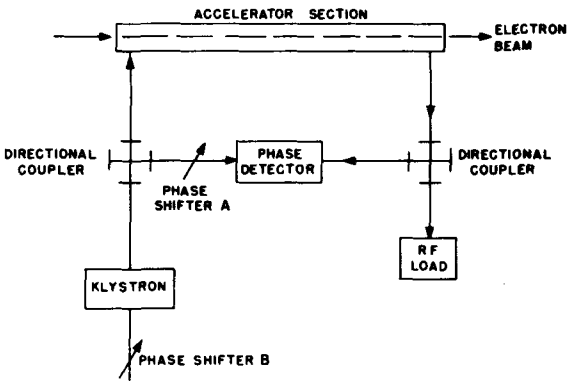

Fig. 16 Method of phasing multi-section accelerator from effect of beam interaction with rf wave. The phasing procedure is as follows: (a) with electron beam off, adjust phase-shifter A for null on phase detector; (b) turn on electron beam and adjust phase-shifter B for null on phase detector.

B. Klystron Specifications

The tentative electrical specifications of the M accelerator klystron are listed in Table 4. Earlier Stanford tubes were of three-cavity design and showed gains of about 30 db. The more extensive and exacting drive system for the 2-mile machine requires a five-cavity tube with a minimum gain of 50 db. Other differences in the electrical specifications of the old and new tubes are described in the following sections of this report.

TABLE 4

Project M Klystron
Tentative Specifications

	Typical operating conditions
Peak forward beam voltage	248 kv
Peak beam current	246 amps
Peak input beam power	61 Mw
Beam voltage pulse length	3.2 μsec
Pulse repetition frequency	360 pps
Average input beam power	71 kw
Frequency	2,856 Mc/sec
Peak drive power	240 watts
Peak rf power output	24 Mw
Average rf power output	21.6 kw
RF output pulse length	2.5 μsec
Efficiency $\left(\frac{\text{peak output rf power}}{\text{peak input beam power}}\right)$	38%
Gain	50 db
Life	2,000 hours

Tentative mechanical specifications have also been determined. To satisfy the requirements of an all-metal vacuum waveguide system between the klystrons and the accelerator, special steel flanges and copper gaskets will be required at the klystron waveguide outputs for connection to the waveguides feeding the accelerator. The easiest mechanical arrangement appears to be one in which the waveguide flanges are in the same plane, resulting in the waveguide outputs being parallel to the tube axis, as shown in Fig. 17. The cylindrical permanent magnet is attached to the klystron body with the pole pieces placed as close to the beam as possible. Not shown on the drawing are the lead radiation shielding around the collector, a steel cylinder to shield the cathode from stray magnetic fields, and several other mechanical details for which designs have not yet been worked out.

C. Aspects of Klystron Design

In general, the design of the klystrons for the 2-mile accelerator has been based on the experience obtained over a period of some 10 years with the klystrons used on the present Stanford Mark III accelerator. We shall now review briefly some of the shortcomings of the Mark III klystron and describe the changes made in designing the new tube.

1. Sealed-off Tube

Although the Mark III klystrons are continuously pumped, there appeared to be no question that a sealed-off high-power klystron could be developed for the 2-mile accelerator. Sealed-off klystrons are in fact commercially available which operate at substantially the same voltage, frequency, and power output as specified for the M klystron. To date, more than a dozen sealed-off high-power tubes have been built at Stanford, and no special difficulty in operation up to full beam power has been observed.

2. Perveance

The Mark III klystron operates with an electron gun of microperveance equal to one. This early tube has over the years shown a tendency to oscillate in the gun region. These oscillations, usually at about 12 cm, are not present in all tubes, but when present they produce undesirable output modulation.

The mechanism of the gun oscillation, although understood in general terms, has not been precisely interpreted. In general, the oscillations appear to be of the Lewellyn diode type, and they can usually be decreased in amplitude or eliminated by appropriate loading of the anode-cathode cavity. It is probable that some additional mechanism is involved in the oscillation, such as rf voltages between the cathode and focusing electrodes, which might actually result in a triode type of oscillation.

In any case, the M klystron has been designed with a microperveance-two gun. The operating voltage for the power output required is approximately 250 kv at microper-

veance two, as against 350 kv for the micro-perveance one of the Mark III klystron; this has resulted in a reduction in total radiation shielding weight. In addition, the micro-perveance-two guns previously tested had not exhibited diode oscillations. To provide ad-

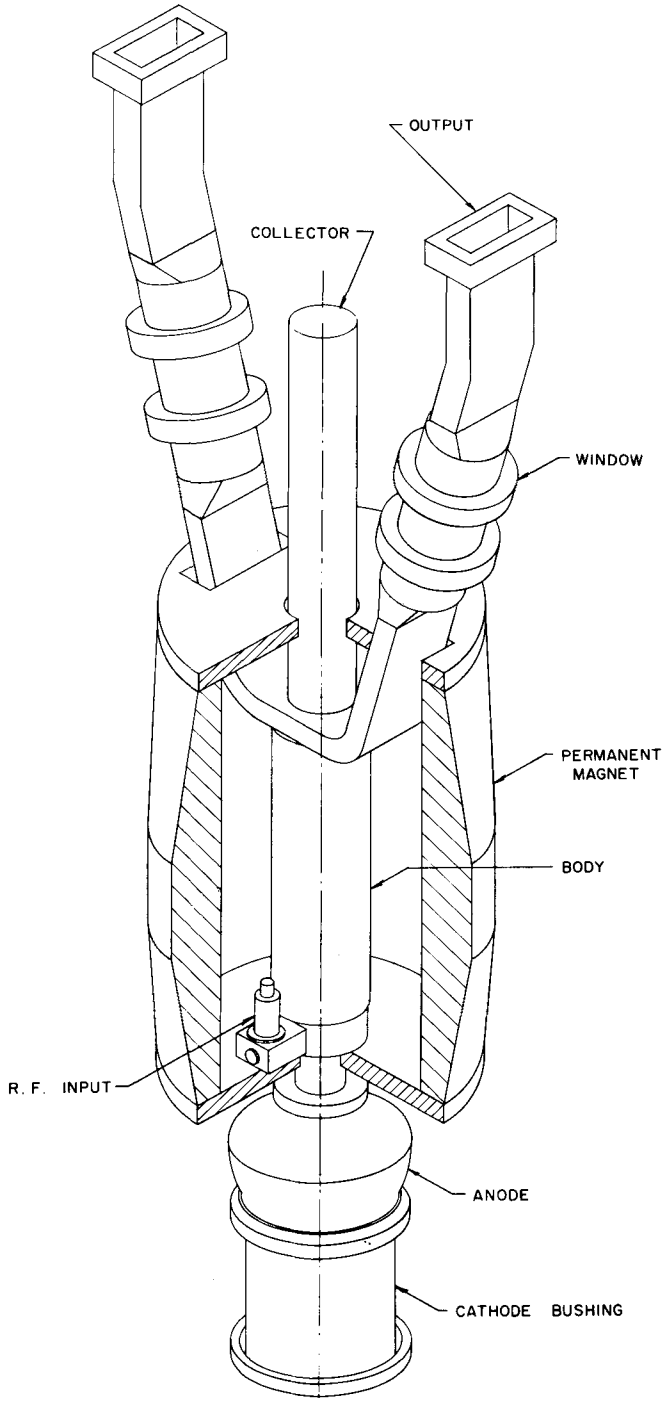

Fig. 17 Project M klystron.

ditional insurance that diode oscillations would not occur, the shape of the anode-cathode region in the new tube has been designed so that it serves as a smooth transmission line into the oil-tank area surrounding the cathode bushing. Thus heavy rf loading of the cavity is obtained by coupling to the lossy oil.

3. Body Design

The Mark III klystron is a three-cavity tube with tunable cavities, and has a total gain of approximately 30 db. One of the problems with this design has been the generation of appreciable harmonic power at ~5 cm wavelength. These 5-cm oscillations were produced by feedback through the drift tubes between cavities, and have been controlled by the use of mode suppressors in the cavities. However, attempts to build four-cavity klystrons with the Mark III cavity design were not successful because of the tendency to oscillate.

In designing the M klystron, it was decided that the cavities need not be tunable. By the use of modified broad-banding techniques, it was possible to design a fixed-tuned five-cavity klystron with an overall length not much greater than that of the original three-cavity Mark III klystron. The dimensional tolerances of the cavities are not critical, and a gain of 50 db is readily attainable. To reduce the possibility of 5-cm oscillations, each of the cavities of the M klystron is of a different shape. As a result, the resonant harmonic frequencies in each cavity are different, and even if harmonic feedback through the drift tube occurs no oscillations should result.

The decision to build a fixed-tuned tube has permitted the design of a very simple body, which is essentially a stack of cylinders and disks of appropriate sizes. The whole tube body can be assembled and brazed in one operation, which should result in inexpensive construction.

4. Peak and Average Power

The peak output power required of the M klystron (24 Mw) is only slightly higher than that of the Mark III tube (~15 Mw). However, the average output power (22 kw) is approximately ten times as large, and thus the collector had to be completely redesigned. The average dc input power to the M tube will be between 60 and 70 kilowatts, and the collector is expected to be able to dissipate up to about 100 kilowatts. The redesigned electron gun results in a cathode loading of about 5 amperes peak per square centimeter, and about 6 milliamperes average per square centimeter. These numbers are conservative; it would appear that a cathode life of the order of 20,000 hours under these loading conditions is quite feasible.

5. Focusing

The Mark III klystron was focused by electromagnets wound directly on the body of the tube. (Industrial tubes have been built so they can be slipped into focusing coils which are permanently mounted in the system.) In the case of the 2-mile accelerator, it was decided that the additional complications of magnet power supplies, interlocks, and water cooling required for electromagnet focusing were such that a study of the possibility of focusing by permanent magnets was warranted.

Three approaches to permanent-magnet focusing are possible: one uses a unidirectional field, much like that of the usual electromagnet focusing of high-power beam tubes; the second uses periodic-field focusing (an extension of the system used extensively in low-power traveling-wave tubes); and the third, a compromise between the first two, uses field-reversal focusing.

The unidirectional field has many advantages from a klystron construction standpoint: it is a direct adaptation of the existing tubes to permanent magnets. Its disadvantage is that the weight and cost of the magnet are the highest of the three cases. The periodic-focusing scheme results, in principle, in a magnet weight inversely proportional to the square of the number of focusing periods. However, the additional difficulties in tube construction necessary to place the pole pieces close to the beam tend to cancel out the saving in magnet cost, and may decrease the ease of repairing the tubes. The main objections to periodic focusing are that the beam-entrance conditions

are critical and that the tube efficiency may vary greatly as the beam voltage is varied.

Progress in magnetic materials in the past few years has made uniform-field focusing quite feasible. Although no M klystrons have yet been tested with permanent-magnet focusing, we have now in the laboratory a permanent magnet weighing less than 400 pounds which produces the field required for operation at about 20 megawatts. With possible slight modifications in the gun structure we should be able to achieve with permanent magnets the performance characteristics required for the M klystron.

To accommodate the permanent-magnet focusing scheme, the tube length has been reduced from the original design; this "short" tube has not yet been tested, but computations indicate that the specified gain and general performance can likely be attained.

6. Klystron Windows

Failure of the output windows presently seems to be the most serious limitation to long-life operation of klystrons in an accelerator application. This application differs from the usual commercial use of klystrons in that the rf load system is evacuated rather than pressurized. Under these conditions, the most common type of failure is formation of many small "pin holes" through the window dielectric. In continuously pumped tubes, this may not be serious as long as the load is kept evacuated. In sealed-off tubes, however, either a sufficiently large number of holes or letting the load down to air will cause failure of the klystron due to excessive gas pressure.

A second type of failure, cracking of the disk due to thermal stress, occurs in some cases. It is always accompanied by puncturing.

The Mark III klystrons have for many years used an alumina disk window, 3 inches in diameter, sealed in a cylindrical "pill box" with suitable transitions and matching irises to rectangular waveguide. For several years, the Mark III windows have been shielded from electrons in the output gap of the klystron by placing two waveguide bends before the window. This resulted in an improvement of mean life by a factor of more than four (one should say half-life, since the failure rate on large numbers of windows is exponential). It is assumed that this has prevented charging of the dielectric by high-energy electrons elastically scattered from the gaps. The energy of these electrons ($\sim$300 kv) is high enough to give gradients through the disk greatly exceeding the dielectric strength if the load side is returned to ground potential in some manner.

Various window designs and dielectric materials have been tried on Mark III, but to date no substantial improvement in life has resulted. These include modifications of the disk structure, conical assemblies, $\lambda/2$ rectangular blocks, slanted disk windows, and double disk windows with evacuation between them (used on the 70-Mev Mark IV machine). Various aluminas made by different manufacturers have been tried in the disk structure.

An evacuated resonant ring has been used for several years to study windows apart from the tube. With this device we can test windows to 30 Mw peak and 35 kw average power, which exceeds M requirements, and far exceeds the $\sim$15 Mw and 2 kw on Mark III. Although several windows have failed in the ring, no combination of conditions has been found which causes predictable failures. However, at 20 Mw peak power we have found X-rays with energies of 100 kv produced at the window.

Bombardment glows are also produced on the surface of the windows. These are of two general types, a bar structure normal to the E field, and a wide strip parallel to the E field. The latter type is associated with overheating, a condition found in some windows. Such windows can usually be made to crack from thermal stress at sufficiently high average power. It is not known why these differences exist among windows of apparently the same construction. These "hot" windows can be operated with pressure in the system without overheating, confirming that the excessive heat is due to particle bombardment.

At present the best explanation for the "pinhole" type of failure involves charging of the disk by electrons produced near the window, followed by discharge on one side due to arcing. Conducting coatings to remove the charge and thicker disks are two approaches being tried to eliminate this problem.

Work is continuing, both at Stanford and in the tube industry, on other designs and materials. Among the promising materials are BeO, quartz, and pyroceram. For the latter two, sealing to metal is a major problem.

7. Output System

During the Stage I operation of the 2-mile accelerator, the power from each klystron will be divided to feed four 10-foot sections of the machine. Under these conditions, it appears reasonable to divide the power output at the klystron so that each window would be subjected to only half the peak and average power; the power would again be divided to feed individual 10-foot accelerator sections. If the power from a single klystron is eventually used to feed only one 10-foot section. the tube can be redesigned to have a single output (assuming that the window problem at full peak and average power has been solved) or else the power outputs can be recombined in a suitable coupler.

D. Klystron Performance

At the present time, more than a dozen M klystron tubes have been built and tested at Stanford. None of these has exhibited any tendency to oscillate, either in the gun region or in the cavities. All the tubes have been operated up to peak power in excess of 20 Mw (see Fig. 18), but lack of test equipment has prevented full average power tests. A tube is now undergoing life test at 200 kv beam voltage and 165 amps beam current at a pulse repetition of 360 pps and a beam pulse length of about 4 μsec. The total rf output is about 10 kw average and 12 Mw peak.

In general, the power divides equally between the two output arms as long as the loads on each arm are equal. The division, however, is a rather critical function of the load characteristics, and further tests are necessary to determine how well the balance can be maintained when accelerator sections are used as the loads.

VIII. MODULATORS

Each klystron connected to the 2-mile accelerator will require a pulsed power input of 64 Mw peak and 74 kw average at a maximum repetition rate of 360 pulses per second. Early studies of modulator systems capable of supplying this power showed the definite economic advantages of the line-type modulator, and thus our entire design effort has been centered in this direction.

The number of klystrons which should be operated from each modulator was considered. This led to the decision to power a single klystron from each modulator for the following principal reasons: (a) the peak pulse power requirement of each klystron is comparable to the highest outputs yet obtained from modulators constructed to operate at the required pulse repetition rate; (b) the replacement of any klystron would require the interruption of power to other klystrons connected to the same modulator; (c) connection of several klystrons to each modulator would cause greater difficulty in obtaining the required pulse amplitude precision.

On the other hand, cost studies supported by technical and operational considerations have shown the advantages of powering a large number of modulators from each dc supply. These factors have led to the decision to oper-

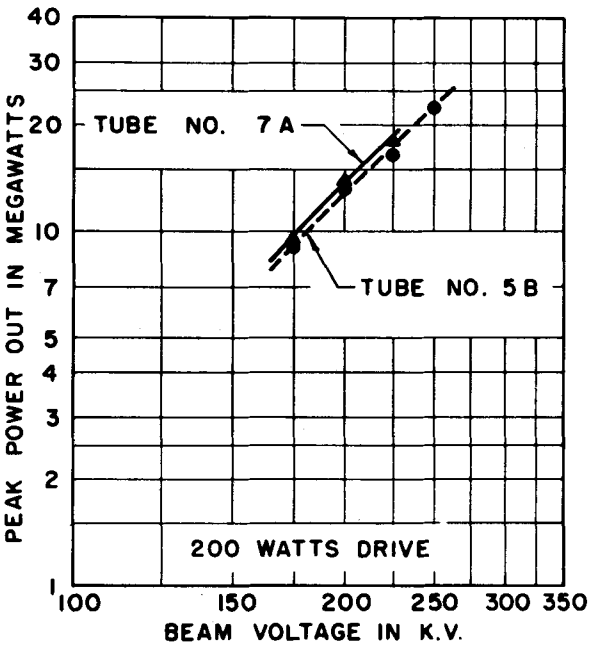

Fig. 18 Typical values of peak power output vs beam voltage for Project M klystrons.

ate 32 modulators from each supply. Thus, 8 dc supplies, each rated at 3 Mw output, are required in Stage I and 32 similar supplies in Stage II to take care of all the modulators connected to the accelerator. Since the design of the dc supplies follows conventional practices, we shall in this report deal further only with the modulators. The over-all requirements of the 2-mile accelerator, and in particular the klystron characteristics, the stability specifications associated with the electron beam energy, and the need for highly reliable 24-hour-per-day service, have led to the modulator specifications shown in Table 5.

TABLE 5

Project M

Modulator Performance Specifications

Peak power output (max)	64 Mw
Average power output (max)	74 kw
Output pulse voltage range	158–248 kv
Output pulse current range	120–258 amps
Load impedance range	1,320–962 ohms
Pulse length (flat top)	2.5 μsec
Rise and fall time (max 0–100%)	0.7 μsec
Pulse repetition rate: (established by control trigger)	60, 120 . . . 360 cps
Pulse height deviation from flatness (max)	±0.5%
Pulse time jitter (max)	±10 mμsec
Pulse-to-pulse amplitude jitter (max)	±0.25%
Pulse amplitude drift:	
a. Long term: The average pulse amplitude is not to deviate more than ±1.5% from nominal setting per hour.	
b. Short term: Pulse amplitude shall not change from nominal value by more than ±0.25% in any 5-minute period.	

The major modulator development problems were the following:

a. To find or develop a pulsed switching device capable of reliably handling the peak and average powers involved, with no more than the specified time jitter.
b. Synthesis of a practical pulse-forming network and design of a pulse transformer capable of meeting the pulse-shape specifications.
c. Development of circuitry and components capable of meeting the pulse amplitude jitter and drift specifications.

Each of the development areas listed above will be briefly described.

A. The Switch

Early studies showed that neither high- nor low-pressure spark gaps nor hydrogen thyratrons were promising for this application. Accordingly, since 1959, efforts have been concentrated on developing the multigrid mercury-pool ignitron as a switch. In brief, the ignitron has been able to meet or exceed all the requirements for this application.[26] Ignitron switches have been tested at powers up to 144 Mw peak and 110 kw average. Pulse-forming networks of various characteristic impedances have been tried experimentally. The final modulator design employs a pulse transformer having a 12:1 turns ratio, a pulse-forming network charged to 41.5 kv (max), and an ignitron switch handling a maximum peak current of 3,100 amperes. While no extensive life-test data are available, we have reason to believe that ignitron life will be very long in this service.

B. The Pulse Shape

To meet the specifications given, two major steps were required, viz., to reduce radically the leakage inductance of the pulse transformer in order to meet the specified rise and decay times, and to develop a practical pulse-forming network capable of generating a pulse flat to ±0.5 percent.

The pulse-transformer requirements were met by using a constant-gradient design, by employing a biased core to fully utilize the range of ΔB of the core material, and by increasing the voltage gradient to 500 volts per mil.

The pulse-forming network is designed around the observation that in the simple theory of transmission lines, no mutual inductance between incremental line segments is considered; yet one of the rigorous solutions of the resulting differential equations is the generation of rectangular voltage pulses. Analytical and experimental studies confirm that, by eliminating the normal mutual inductance between sections, a superior pulse shape can be obtained. We have therefore abandoned the "E" type network based on Guillemin's synthesis.[27]

The pulse-forming network contains 24 sections of equal capacity tapered in impedance

to compensate for the droop introduced by the pulse transformer. To indicate the practicality of the design, it may be remarked that individual capacitors can go out of tolerance by ±2 percent before the pulse shape goes out of tolerance by ±0.5 percent. The capacitors chosen use polyethylene dielectric material rather than paper to reduce losses and because of the better temperature stability afforded by this material.

C. Pulse Amplitude Jitter and Amplitude Drift

Our present system design contemplates the use of induction voltage regulators at each of the eight 3 Mw dc power supplies, both for adjustment of power level and to compensate long-term line-voltage drift.

To accommodate fast line-voltage transients, and to control the voltage to which the pulse-forming network is charged to an accuracy better than the 1 percent afforded by the induction voltage regulators, a "de-Q'ing" circuit[28] (modified* to scavenge rather than dissipate the energy stored in the charging reactors) has been developed. The operation of this circuit may be understood in a qualitative way by reference to Figs. 19 and 20. A sample $kv_1(t)$ of the charging voltage is compared to a reference voltage by the circuit labeled "cf". When the two are equal the thyratron regulator switch conducts at time t_r corresponding to the desired network voltage v_n. In effect, this action shorts the charging reactor, thus preventing further transfer of charge to the pulse-forming network.

Instead of employing a conventional charging reactor, however, the circuit uses a 1.5:1 transformer (called a "transactor") connected with the polarity shown. When the regulator switch closes, $i_2(t)$ flows in such a direction as to recharge the filter capacitor C_1. By this means, and for our conditions, as much as 3 kw of average power can be saved per modulator. The purpose of diode D_1 is merely to relieve the peak inverse requirements on the regulator switch.

D. DC Disconnect

A word about the dc disconnect problem may be appropriate. The short-circuit capacity of the 3 Mw supplies will be on the order of 10^4 amperes. In order to protect the system against short-circuited components to the right of the filter section (Fig. 19), the filter capacitor C_1 is split into two equal 5 μf sections, thereby making it possible to interrupt the circuit with a fast switch S_2 without requiring the switch to handle the full short-circuit current. Shorted components in and to the left of the filter section requires the backup of a fuse (F), however.

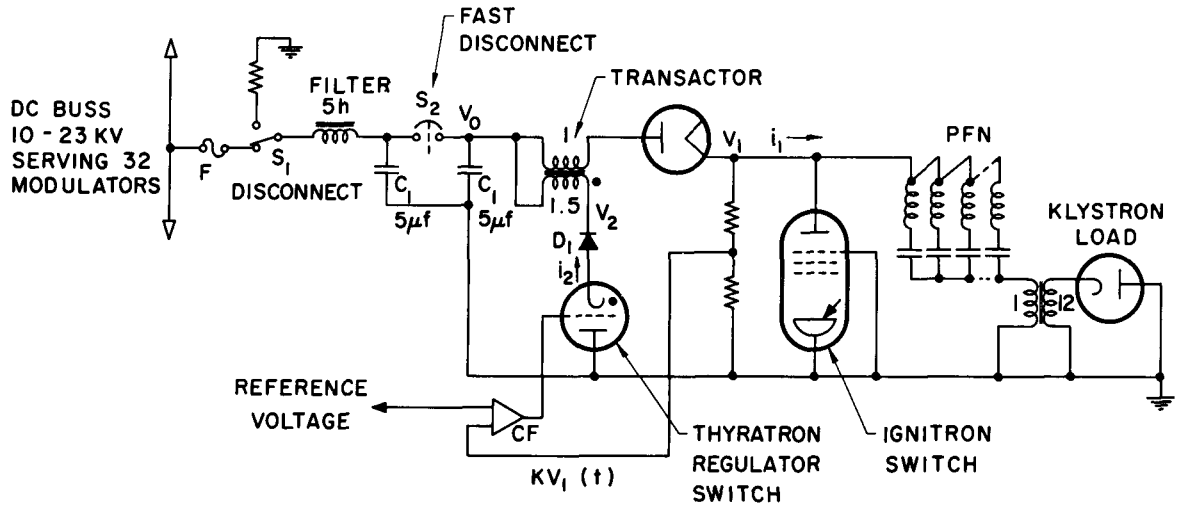

Fig. 19 Modulator schematic showing power-scavenging pulse-to-pulse voltage regulator circuit.

* This development was carried out by the RCA Missile and Surface Radar Division (Moorestown) under contract to Stanford.

IX. RESEARCH PLANNING

A. Introduction

A space of approximately 3,000 by 2,000 feet is available for the target facilities of the 2-mile accelerator, and it should be possible to have separate areas for different types of experiments. Originally it was believed that the experimental program of the accelerator should have as its primary concern experiments such as photo-production and electron scattering. Yields of secondary particles had been estimated as approximately 5 to 10 times greater than those of the CERN and Brookhaven AGS accelerators, and it was felt that these yields were not large enough to make secondary-particle work a very important part of the research program. However, recent calculations by Ballam and Drell [29,30] indicate that the yields of high-energy secondaries should be over 100 times those of existing accelerators; as a result, we have changed our planning considerably.

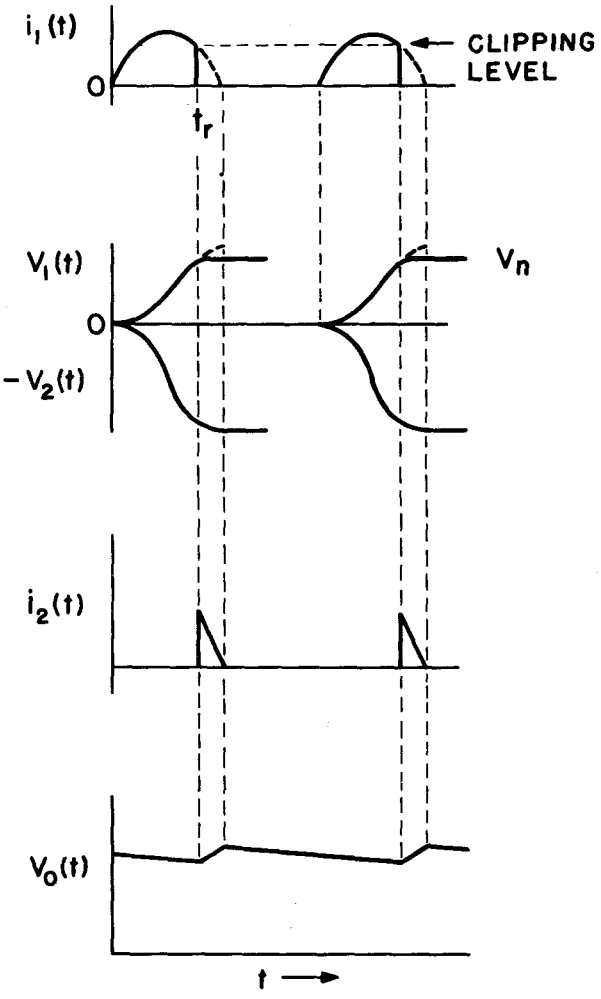

Fig. 20 Current and voltage waveforms associated with pulse-to-pulse voltage regulator circuit.

Special particle-detection problems are caused by the duty cycle of about 6×10^{-4} (360 pps and $\sim$1.7 μsec pulse length), which is smaller than that of circular accelerators. The short duty cycle favors experimental techniques that use momentum analysis, since these reduce the total number of background particles passing through the detectors.

The low duty cycle does make possible the more economic use of rf separators, and the high accelerator frequency of 2,856 megacycles/sec makes flight paths for such separators reasonably short without additional modulation of the beam. These separators may play an important role in the secondary-beam experiments. The possibility of making an rf-modulated photomultiplier also seems interesting for use with photo-production and electron-scattering experiments.

B. Secondary Particle Beams

It is obvious that the 2-mile accelerator has special characteristics which will make the use of secondary-particle beams considerably different from those produced by circular proton accelerators. The most obvious characteristic is that the beam is pulsed 360 times a second. Since bubble chambers are presently operated at about 1 pulse per second, the yield available to a bubble chamber is no greater even for high-energy secondary particles than the yields from the AGS and CERN machines, while for low-energy secondaries these accelerators will have even greater relative yields. The production mechanism for electrons is quite different, however, and as a result the Stanford machine will produce higher yields for certain types of particles. For example, large numbers of muons can be made directly by electromagnetic pair production. In addition, the Drell-Ballam mechanism predicts a good yield for any particle that has either charge or magnetic moment and that, in addition, interacts

strongly with nucleons. A spark chamber would be a good match to the 2-mile accelerator since it could be pulsed at the same repetition rate.

With regard to bubble chambers, there is one significant advantage: a pulse every second or so can be given to a bubble chamber without appreciably affecting the other experiments which use the 360-cycle pulse rate. To do this, of course, the accelerator must be designed in such a manner that the beam can be shifted in energy and from one target area to another between pulses.

It is apparent that there would be many advantages in having two types of secondary-beam facilities: one for bubble chamber work where only one pulse or so a second can be used, and the other for experiments which can use the entire beam.

C. Electron Scattering Experiments

The shielding problems will be quite different for thin and thick targets. With a 60 microamp beam of 40 Bev electrons incident on an unshielded 20 cm target of liquid hydrogen (a thin target), the estimated neutron flux is about 100 times general population tolerance at 1,000 feet. This compares with estimates of about 10^7 times tolerance for a case where the total energy of the incident beam is absorbed. As a result, for the first case, a relatively simple configuration can be used with, for example, a thick concrete pill-box structure shielding the interaction region. The scattered electrons could then pass through a reasonably large opening in this structure into an external unshielded magnetic-analysis system. If, on the other hand, a similar experiment were attempted with a thick target, where an attenuation of about 10^7 is required, an opening one-half inch in diameter would be the maximum possible in the 35-foot-thick shielding wall.

D. Photon Beam Areas

It is very difficult to produce a clean beam of X-rays without allowing a large number of background particles produced in the radiator to pass through the target region. A study by Kenney[31] indicates that a collimation system at least 100 feet in length would be required at 45 Bev. Moreover, a similar distance is required if the primary electron beam is not to be allowed into the target area, or at least to be kept several feet away from the target. As a result, it appears possible that, for cost reasons, a system with much smaller beam clearance (1 or 2 feet) may be used, and that one will try to live with the large background from the radiator. However, the problem of background from the area where the electron beam is to be stopped must be solved. It is desirable that there be at least 25 feet of concrete between this region and any counting equipment. All of the problems are complicated by the very high beam current (there will be as much as 2.4 megawatts of power in the electron beam; a good X-ray beam may contain about 100 kilowatts). As a result, to stop the electron beam will require about 20 feet of water-cooled absorber.

E. Low Radiation Experiments

There are some types of experiments, primarily those involving positrons, which may produce very small amounts of radiation. Positron beams have been produced on the present Stanford 1 Bev accelerator with an intensity of about 10^{-4} that of the primary beam.[32] This is done by introducing a radiator into the electron beam at an energy of about 300 Mev. From the shower of secondaries produced, positrons of about 8 Mev are focused and then accelerated by reverse-phasing the remaining portions of the accelerator. A similar beam could be produced on the Project M accelerator and, for example, positron-scattering experiments could be done in a relatively unshielded area if the positron beam itself is absorbed under shielding.

A possibility that has been explored by Cassels[33] is that of making a monochromatic X-ray beam by the annihilation of positrons in flight. Unfortunately, this beam would not be completely monochromatic since it is impossible to avoid bremsstrahlung production by the positrons in the material in which they annihilate. However, such a beam may be much more effective than photon-difference

methods for establishing the energy of the X-rays in photoproduction experiments.

If a spark chamber is to be used to obtain a very large solid angle, more or less completely surrounding the photon or electron interaction region, only a very low-intensity electron or photon beam could be used because electromagnetic interactions would completely swamp the chamber at high intensity. This would be true in spite of the fact that the primary beam is not allowed to pass through the chamber itself. However, the large solid angle available could in many cases more than compensate for the low usable intensity.

F. Low Energy Experimental Areas

If it is felt desirable to use the Project M accelerator extensively at lower beam energies ($\sim$ 5 Bev), a special area should be built since the shielding and experimental problems would be quite different from those in the higher energy region. For example, it might be possible to completely enclose a target facility with shielding at this energy region, while at the 40 Bev region it would be prohibitively expensive to enclose the $\sim 10^5$ square-foot area required.

G. Facilities Planned for Project M

Initially, we are considering the construction of only two areas. One of these will be for all secondary-particle experiments by bubble chambers and counters, while the other will be devoted to electron and photon-beam experiments. However, beam-transport systems will be stubbed in to allow an expansion to 5 or more areas without interfering with the operation of the areas already constructed. It is planned to separate all areas sufficiently so that they can be expanded considerably without interference and in such a manner that the radiation from one will not be a hazard in any of the others. The arrangement of these areas is to some extent determined by the beam-handling problems. To place alternate pulses of the accelerator into different target areas is desirable, and this requires a pulsed deflection magnet. To obtain a deflection of approximately 1 foot with a power transfer capacity of about 1 megawatt requires a 100-foot distance for a 45 Bev beam. A primary consideration in the design of the main beam-deflection system is the desire to have a completely achromatic system, carrying a parallel beam to a deflected parallel beam; in addition the condition is imposed that the deflection system be isochronous, that is, that the path length for electrons of different energies be the same. The configuration shown in Fig. 21 will achieve this. The two quadrupole magnets $Q1$ and $Q2$ bring the beam to a focus at a plane of symmetry. Before reaching this plane the beam passes through a deflection magnet to produce energy dispersion. At the plane of symmetry, energy-defining slits can be introduced; although the slit material will not absorb the beam, it will cause radiation and energy loss from those electrons which pass through it while the desired portion of the beam passes through the center of the slits. Another quadrupole magnet $Q3$ is located at the plane of symmetry of this system in order to make all trajectories normal to the plane. The total angle of deflection which can be produced by such a system cannot be larger than about 30° without causing appreciable path-length differences for particles of different energy. The angles are also restricted for economic reasons, since at 40 Bev it will cost at least $10,000 per degree of beam deflection.

The beam will then be run into a heavily shielded target area. In the case of secondary-beam production one would consider running it through one or two radiation lengths of beryllium and then into a beam absorber. There is little reason for having more than two radiation lengths of material, since one gains only in the low-energy portions of the spectrum

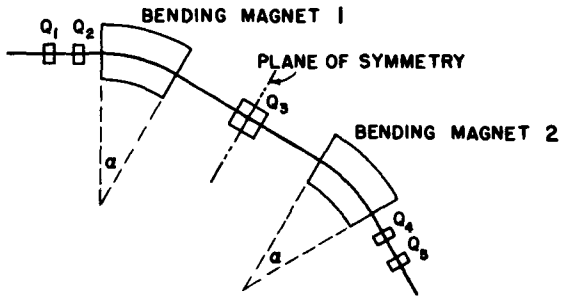

Fig. 21 Beam deflection system.

produced and adds considerably to the problem of getting secondaries out of the target. The problem of secondary-beam production is complicated by the fact that all of the beams come out of the target at mean angles of about mc^2/E, where E is the energy of the secondary and m is its rest mass, and there is a considerable problem in separating these particles from the primary beam. However, there is the advantage that one can choose angles in such a manner as to discriminate in favor of the particles wanted.

The whole target region, beam absorber, and the first analyzing magnet must probably be completely surrounded with very heavy shielding. It would be planned that several particle beams pass through the walls of this enclosure to be further analyzed by external magnetic equipment. For a reasonable portion of their continued flight path, the beams must remain under shielding since very large radiation attenuation is required. If rf separators are to be used, a flight distance of, for example, 600 feet is required to separate k's from p's, π's and positrons at 10 Bev/c. Large handling equipment is required for this area, but it is apparent that it is prohibitively expensive to cover the entire experimental region with cranes or even with buildings. The present plan is to cover only a nucleus of the highest density of shielding and equipment with a building and crane. For example, we plan for this facility a building of about 100×100 feet with a 100-ton capacity crane. This building will then be surrounded with a large parking-lot type of area in which secondary-particle experiments can be conducted, with the building itself serving as a nucleus from which the water lines and power would originate. The crane coverage in the parking lot would be handled by mobile equipment, while the experiments would be housed in relatively simple structures. For example, the use of truck trailers is being considered for the counting equipment.

For the electron-scattering and photon-beam areas, the beam will be deflected similarly to the other side of the main beam line, and a building of at least 100×300 feet is contemplated.

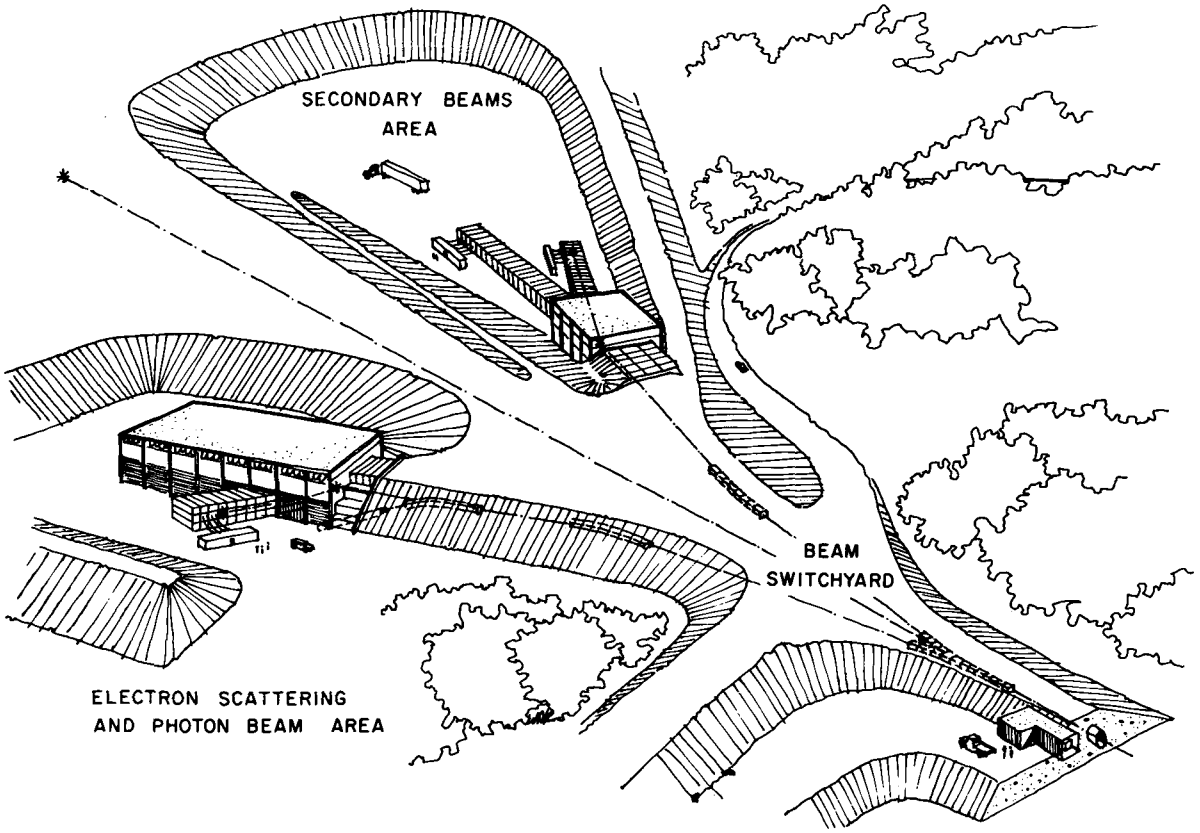

Fig. 22 Tentative layout of the research area for the 2-mile machine. Two target areas will be developed initially.

Again, this building will be only a nucleus and will be surrounded by a parking-lot type of area for at least 100 feet on each side. These areas are sketched in Fig. 22. It is planned that further areas will be placed on either side of the accelerator beam line downstream from the two areas shown.

In addition to the shielding required in the target areas, there will be a large earth barrier 50 feet high and 400 feet thick enclosing the region within about 45° on either side of the main beam line. The major purpose of this barrier is to absorb the very intense muon beams which can be made by the accelerator. A 40-Bev muon has a range of about 400 feet in earth, and although it is not necessarily planned to have any muons incident on this barrier, we believe that it is necessary to have this additional shielding in case a mistake is made in the handling of shielding in the target areas.

REFERENCES

1. R. B. NEAL and W. K. H. PANOFSKY, *CERN Symposium Proceedings*, Vol. 1, pp. 530 ff, CERN, Geneva (1956).
2. *Proceedings of the International Conference on High Energy Accelerators and Instrumentation*, CERN, Geneva (1959): Stanford Two-Mile Linear Electron Accelerator, pp. 369 ff; Beams from High Energy Linear Accelerators, p. 427.
3. See, for example, J. BALLAM *et al.*, Some Aspects of Target Area Design for the Proposed Stanford Two-Mile Linear Electron Accelerator, M Report No. 200, Project M, Stanford University, Stanford, California (Summer 1960).
4. M. G. KELLIHER and R. BEADLE, *Nature* 187, No. 4743, p. 1099 (1960).
5. J. F. STREIB, Report No. HEPL-104, W. W. Hansen Laboratories of Physics, Stanford University, Stanford, California (November 1960).
6. R. B. NEAL, "A high energy linear electron accelerator", M. L. Report No. 185, W. W. Hansen Laboratories of Physics, Stanford University, Stanford, California (February 1953).
7. M. CHODOROW *et al.*, "Stanford high-energy linear electron accelerator", M. L. Report 258, W. W. Hansen Laboratories of Physics, Stanford University, Stanford, California (February 1955).
8. R. B. NEAL, "Design of linear electron accelerator with beam loading", M. L. Report No. 379, W. W. Hansen Laboratories of Physics, Stanford University, Stanford, California (March 1957).
9. R. B. NEAL, "Transient beam loading in linear electron accelerators", M. L. Report No. 388, W. W. Hansen Laboratories of Physics, Stanford University, Stanford, California (May 1957).
10. R. B. NEAL, "Theory of the constant gradient linear electron accelerator", M. L. Report No. 513, W. W. Hansen Laboratories of Physics, Stanford University, Stanford, California (May 1958).
11. R. B. NEAL, "Comparison of the constant gradient and uniform accelerator structures", Project M Report No. 259, Stanford University, Stanford, California (March 1961).
12. M. L. Report No. 612, W. W. Hansen Laboratories of Physics, Stanford University, Stanford, California (May 1959).
13. M. L. Report No. 557, W. W. Hansen Laboratories of Physics, Stanford University, Stanford, California (November 1958)
14. M. L. Report No. 581, W. W. Hansen Laboratories of Physics, Stanford University, Stanford, California (February 1959).
15. M. L. Report No. 520, W. W. Hansen Laboratories of Physics, Stanford University, Stanford, California (July 1958).
16. M. L. Report No. 504, W. W. Hansen Laboratories of Physics, Stanford University, Stanford, California (April 1958).
17. Project M Report No. 246, Stanford University, Stanford, California (January 1961).
18. Project M Report No. 232, Stanford University, Stanford, California (November 1960).
19. R. B. NEAL, "Drive Line Considerations for Project M", M Report No. 105, Project M, Stanford University, Stanford, California (December 1958).
20. G. A. LOEW, "Requirements for a Possible Coaxial Drive System for Project M", M Report No. 107, Project M, Stanford University, Stanford, California (October 1959).
21. R. B. NEAL, "Note on Phase Shift in Transmission Lines Due to Ionizing Radiation", M Report No. 106, Project M, Stanford University, Stanford, California (October 1959).
22. D. GOERZ and R. B. NEAL, "Method of Phasing a Long Linear Electron Accelerator", M. L. Report No. 550, W. W. Hansen Laboratories of Physics, Stanford University, Stanford, California (October 1958).
23. M Report No. 101, Project M, Stanford University, Stanford, California (November, 1958).
24. G. A. LOEW, "Non-Synchronous Beam Loading in Linear Electron Accelerators", M. L. Report No. 740, W. W. Hansen Laboratories of Physics, Stanford University, Stanford, California (August 1960).
25. D. GOERZ and R. B. NEAL, "Phasing a Linear Accelerator from RF Phase Shift due to Beam Loading Interaction", M Report No. 103, Project M, Stanford University, Stanford, California (December 1958).
26. T. F. TURNER and H. S. BUTLER, M Report No. 257, Project M, Stanford University, Stanford, California (March 1961).
27. G. N. GLASOE and J. V. LEBACQZ, *Pulse Generators*, M.I.T. Series, Radiation Laboratory, Vol. 5, pp. 200–203 (1948).

28. R. G. SHOENBERG, "High Power Pulse System Regulation", *Proceedings of the Sixth Symposium on Hydrogen Thyratrons and Modulators*, U. S. Army Signal Research and Development Laboratory, Fort Monmouth, New Jersey (1960).
29. J. BALLAM, "Computation of Secondary-Particle Yields from High-Energy Electron Accelerators", M Report No. 200-8, Project M, Stanford University, Stanford, California (August 1960).
30. S. D. DRELL, "Production of Particle Beams at Very High Energies", M Report No. 200-7A, Project M, Stanford University, Stanford, California (August 1960).
31. R. KENNEY, "Some Considerations in the Design of a Target Area for Photon-Beam Experiments", M Report No. 200-15, Project M, Stanford University, Stanford, California (September 1960).
32. J. PINE and D. YOUNT, Private Communication.
33. J. CASSELS, "Monochromatic Photons at Gev Energies from Positron Annihilation", M. Report No. 200-4, Project M, Stanford University, Stanford, California (June 1960).

DISCUSSION

D. ROBERTSON: Professor Panofsky mentioned that these mixed modes were responsible for beam blowup. I wonder if he would mind enlarging a little on that—mainly whether they are backward-traveling waves or not.

G. A. LOEW: We have done some cold tests and it looks as if they would be backward-wave modes propagating at about 4.3 kMc, or so, and our results are outlined in the paper. We have not detected their generation in the structure by the electron beam because we have never had enough current to get the oscillations started.

L. B. MULLETT: It is rather a pity that Miller from A.E.I. isn't here because he has had some recent experience on the Hamburg injector which is quite relevant. They have, indeed, found this frequency of 4,400 Mc, or thereabouts. They have checked, by low-power measurements, that this is indeed a backward wave so that you have built-in feedback in the system. They haven't exactly tracked down what mode it is but it seems fairly obvious that it is a combination of E and H modes with a cancellation of one component so as to leave a residual transverse deflection. The problem certainly seems to be solved. At A.E.I. and Vickers Research, they have tried a variation of parameters along the length of the waveguide and this works, but, A.E.I. have also discovered that if you put in a center section which is a kind of half-wave transformer, so that it introduces a π phase shift for the unwanted mode, you can suppress the buildup of the unwanted mode over quite a long section.

G. K. O'NEILL: Do you have the flexibility of increasing the pulse length at the sacrifice of peak energy for some experiments?

W. K. H. PANOFSKY: No.

L. BURNOD: When you speak about constant gradient linacs do you mean with or without beam loading?

W. K. H. PANOFSKY: The graph which was shown in my slide corresponds to the case where the unloaded guide would give an increasing gradient but under 10 percent loading would give very closely a uniform gradient.

P. M. LAPOSTOLLE: You mentioned the 10 percent beam loading for your machine. I would like to know what is the main reason for this number and whether you consider that a higher beam loading is really something very difficult.

W. K. H. PANOFSKY: The 10 percent figure is fairly arbitrary. We studied a large number of alternate structures. As you know, there is a trade-off between the steepness of the loading characteristic and the open circuit, the no-loading voltage which you can get. This represents a compromise where we sacrifice approximately 10 percent of the no-loading voltage in order to have only a 10 percent decrease in voltage at the maximum of current which we think makes sense for this kind of an accelerator from the point of view of targeting. Ultimately, in the Phase-II machine, we are talking of over 2 megawatts of beam power. So, from the point of view of various problems, there are some limits. On the other hand, this particular structure could be loaded much more heavily. As an example, one of the applications of this machine is acceleration of a positron beam. Recently Dr. Pine and his students, on the Mark-III accelerator, have accelerated positrons with an intensity of approximately 10^{-4} times that of the electron beam. The way you do that is to put a converter part way up the machine and reverse phase the rest of the machine. Now in that case, obviously if one did something of this kind with this machine, in the section ahead of the converter you would like to get as much current as you can stand because the degeneration of the spectrum doesn't make any difference. Under those circumstances loading heavier than 10 percent is certainly indicated. However, there are very serious problems with the radioactivity associated with the converter and the downstream section from the converter. The theory has not been studied in enough detail to know whether such higher loading in the first part of the machine would, in fact, be useful. To answer your questions in one sentence: the loading decisions are reasonably arbitrary.

J. B. ADAMS: I don't exactly know how to put this question. What I want to get at is the amount of effort in a high-intensity machine of this sort that has to go into the problems of targeting and using the machine. Now I believe that, at Stanford, you have put a tremendous amount of thought into this. Can you give any indication of, for example financially, how much money goes into the accelerator, how much in the beam handling area at the far end. I think this is very relevant to the high-intensity machines that are being discussed at the moment and, as far as I know,

Stanford is the only place where serious thought is being put into this.

W. K. H. PANOFSKY: I think you overstate considerably the amount of serious thought which is being given to it at Stanford. I think "worry" is more the right term than "thought". The situation is as follows. Approximately 10 to 15 percent of total construction funds is allocated in that direction, at the present moment, and a rather substantial fraction of the research and development funds. We have done, I think, somewhat more work than is customary at this stage. We have worried about targeting, we have worried about secondary-beam sources and how to cool them and how to live with them. We have worried a great deal about the problem of long range skyshine even though there are no really good calculations. I can give you an example of the kind of numbers which I think are a warning to people in high-energy machines. If we take our full beam and run it through a liquid hydrogen target of about 10 inches in length, then the fraction of the solid angle from such a target which can see open space must not be larger than 1 percent of a sphere in order not to exceed what we call the mega-body-dose at distances of 1,000 feet, or more, through skyshine. If, on the other hand, the same beam would hit a lead brick rather than the hydrogen target, and we let 1 percent of the photoneutrons look into the outside, then we would exceed by a factor of 10^5 the mega-body-dose at a distance of 1,000 feet. Now electrons make, on the average, only 1 percent as many neutrons per particle as protons. This means that, excepting for well-controlled thin-target hydrogen experiments, one is forced to confine secondary beams to a closed area. The main thing which we have done is to leave a great deal of flexibility.